**HYDRODYNAMIC RADIATIVE TRANSFER PROCESS AROUND ACTIVE GALACTIC NUCLEI**

**BY**

**Mihiret Mekonen**

**Advisor: Tolu Biressa(PhD)**

A THESIS SUBMITTED TO THE GRADUATE STUDIES OF JIMMA UNIVERSITY IN PARTIAL FULFILLMENT OF THE REQUIREMENT FOR THE DEGREE OF MASTER OF SCIENCE IN PHYSICS (ASTROPHYSICS)

At

JIMMA University

College of Natural Sciences

Jimma, Ethiopia

June, 2024

**APPROVAL SHEET**

JIMMA UNIVERSITY

COLLEGE OF NATURAL SCIENCE

DEPARTMENT OF PHYSICS

As advisor(s)/Examiner, I/We here certify that I/We have read the proposal prepared by Mihiret Mekonen under my/our guidance, which is entitled **HYDRODYNAMIC RADIATIVE TRANSFER PROCESS AROUND AGN** , in its final form and have found that its format, citations and bibliographical style are consistent and acceptable and fulfill the university and department style requirements.

| | | |
|---|---|---|
| Tolu Biressa(PhD) | ________ | ________________ |
| Advisor | Signature | Date |
| Dr.Tolu Biressa(PhD) | ________ | ________________ |
| H.Department | Signature | Date |
| Menberu Mengesha (Proffesor) | ________ | ________________ |
| Examiner | Signature | Date |

**DECLARATION**

JIMMA UNIVERSITY
COLLEGE OF NATURAL SCIENCE
DEPARTMENT OF PHYSICS

I here by declare that this MSc thesis is my original work and has not been presented for a degree in any other university, and that all sources of material used for the thesis have been duly acknowledged.

AUTHOR: Mihiret Mekonen
TITLE: HYDRODYNAMIC RADIATIVE TRANSFER PROCESS AROUND ACTIVE GALACTIC NUCLEI
DEPARTMENT: Physics
DEGREE: M.Sc.
Convocation: June, 2024

Permission is herewith granted to Jimma University to circulate and to have copied for non-commercial purposes, at its discretion, the above title upon the request of individuals or institutions.

| Mihiret Mekonen | ____________ | ____________________ |
| --- | --- | --- |
| Author | Signature | Date |

**Table of Contents** . . . . . . . . . . . . . . . . . . . . . . . . . . . . i

**List of Figures** . . . . . . . . . . . . . . . . . . . . . . . . . . . . . iii

Abstract . . . . . . . . . . . . . . . . . . . . . . . . . . . . . . . . . iv

Acknowledgment . . . . . . . . . . . . . . . . . . . . . . . . . . . . . vi

**1 Introduction** **1**

1.1 Background and Literature Review . . . . . . . . . . . . . . . . . . . . . . 1

1.2 Statement of the problem . . . . . . . . . . . . . . . . . . . . . . . . . 3

1.3 Objectives . . . . . . . . . . . . . . . . . . . . . . . . . . . . . . . 4

1.3.1 General objective . . . . . . . . . . . . . . . . . . . . . . . 4

1.3.2 Specific objectives . . . . . . . . . . . . . . . . . . . . . . 4

1.4 Methodology . . . . . . . . . . . . . . . . . . . . . . . . . . . . . . 5

1.5 Limitations of the study . . . . . . . . . . . . . . . . . . . . . . . . . 6

1.6 Ethical considerations . . . . . . . . . . . . . . . . . . . . . . . . . . 6

**2 Active Galactic Nuclei and its Environment** **7**

2.0.1 Seyfert Galaxies . . . . . . . . . . . . . . . . . . . . . . . . 8

2.0.2 Quasars . . . . . . . . . . . . . . . . . . . . . . . . . . . . 9

2.0.3 Radio Galaxies . . . . . . . . . . . . . . . . . . . . . . . . 10

2.0.4 Blazars . . . . . . . . . . . . . . . . . . . . . . . . . . . . 11

2.1 Structure and Composition of AGN . . . . . . . . . . . . . . . . . . . . . 11

2.1.1 Accretion Disk . . . . . . . . . . . . . . . . . . . . . . . . 12

2.1.2 Broad-Line Region (BLR) . . . . . . . . . . . . . . . . . . . . . . . . . 13
2.1.3 Narrow-Line Region (NLR) . . . . . . . . . . . . . . . . . . . . . . . . 14
2.1.4 Dust Torus . . . . . . . . . . . . . . . . . . . . . . . . . . . . . . . . . 14
2.1.5 Jets . . . . . . . . . . . . . . . . . . . . . . . . . . . . . . . . . . . . 15
2.2 Unified Model of AGN . . . . . . . . . . . . . . . . . . . . . . . . . . . . . 15

**3 AGN Radiation Model and Its Effects on Its Environment 19**
3.1 Accretion process . . . . . . . . . . . . . . . . . . . . . . . . . . . . . . . 19
3.2 Radiation model . . . . . . . . . . . . . . . . . . . . . . . . . . . . . . . . 22
3.2.1 Emission . . . . . . . . . . . . . . . . . . . . . . . . . . . . . . . . . 22
3.2.2 Emission Lines . . . . . . . . . . . . . . . . . . . . . . . . . . . . . . 25
3.2.3 Collimation . . . . . . . . . . . . . . . . . . . . . . . . . . . . . . . . 26
3.2.4 Absorption and Scattering . . . . . . . . . . . . . . . . . . . . . . . . 27
3.2.5 Re-emission . . . . . . . . . . . . . . . . . . . . . . . . . . . . . . . . 29
3.3 Radiation and the Dusty Torus . . . . . . . . . . . . . . . . . . . . . . . . 30
3.4 AGN Effects on its Environment . . . . . . . . . . . . . . . . . . . . . . . 30
3.4.1 Suppressive Effects . . . . . . . . . . . . . . . . . . . . . . . . . . . . 30
3.4.2 Triggering Effects . . . . . . . . . . . . . . . . . . . . . . . . . . . . . 31
3.4.3 Environmental dependence . . . . . . . . . . . . . . . . . . . . . . . . 32
3.4.4 AGN feedback . . . . . . . . . . . . . . . . . . . . . . . . . . . . . . . 33

**4 Relativistic Hydrodynamic Radiative Transfer Equations 34**
4.1 General Relativity and Exact Solutions to Einstein Field Equations . . . . 34
4.1.1 Schwarzschild Metric . . . . . . . . . . . . . . . . . . . . . . . . . . . 36
4.1.2 Kerr Metric . . . . . . . . . . . . . . . . . . . . . . . . . . . . . . . . 38
4.2 Radiative Transfer Equation . . . . . . . . . . . . . . . . . . . . . . . . . . 42
4.2.1 Pressure supported accretion tori . . . . . . . . . . . . . . . . . . . . 45

**5 Result and Discussion 50**
5.1 Structure of AGN in kerr space time . . . . . . . . . . . . . . . . . . . . . 50

5.1.1 Relativistic Equation of Motion in Kerr-Newman Spacetime . . . 54
5.2 Accretion as the Main Source of Energy Release from Active Galactic Nuclei 58
5.2.1 Potential Contributions of Nuclear Fusion in AGNs . . . . . . . . . 60
5.2.2 Density and Temperature profile of an AGN . . . . . . . . . . . . . 62
5.3 Radiation Transfer from AGN to Host Galaxy . . . . . . . . . . . . . . . . . 63
5.3.1 Emissions, Both Thermal and Non-Thermal, in the Temperature Range of $10^5$–$10^7$ Kelvin . . . . . . . . . . . . . . . . . . . . . . . . 64
5.4 The effect of Radiative hydrodynamic transfer on the Energy output of host galaxy . . . . . . . . . . . . . . . . . . . . . . . . . . . . . . . . . 65
5.4.1 Accretion Efficiency and Its Influences on the Energy output of the Host Galaxy . . . . . . . . . . . . . . . . . . . . . . . . . . 65
5.4.2 The Influence of Optical Depth on the Energy out put of the Host Galaxy . . . . . . . . . . . . . . . . . . . . . . . . . . . . . . . . 67

**6 Summary and Conclusion** **70**

**Bibliography** . . . . . . . . . . . . . . . . . . . . . . . . . . . . . . . . . . 70

# List of Figures


2.1 Structure of active galactic nuclei (Image Credit: Matt Perko, UCSB)). . . 12
2.2 Schematic representation of the unified AGN model (Credit: Beckmann & Shrader 2012) [1] . . . . . . . . . . . . . . . . . . . . . . . . . . . . . . . . 16

5.1 Visualization of the Kerr Metric Components for a Rotating Black Hole . 51
5.2 Visualization of the Kerr-Newmann Metric Components for a Rotating Black Hole . . . . . . . . . . . . . . . . . . . . . . . . . . . . . . . . . . 52
5.3 The amount of radiation processed at the event horizon . . . . . . . . . . 58
5.4 Comparison of viscous dissipation energy and nuclear fusion energy in AGN . . . . . . . . . . . . . . . . . . . . . . . . . . . . . . . . . . . . . 61
5.5 Temperature and density of an AGN . . . . . . . . . . . . . . . . . . . . . 63
5.6 Theoretical thermal and non-thermal emission spectrum of an AGN. . . 64
5.7 Accretion Efficiency Influence on the Energy output of the Host Galaxy . 66
5.8 Impact of Optical Depth on Specific Intensity Change . . . . . . . . . . . 68
5.9 Impact of Dust on Specific Intensity Change . . . . . . . . . . . . . . . . . . 69

# Abstract

This thesis investigates the physical processes governing Active Galactic Nuclei (AGNs) and their interaction with surrounding environments, focusing on the interplay of hydrodynamics and radiative transfer. The model equations used were that of the standard AGN models rooted in Einstein General Relativity. The study aims to understand radiation emission and absorption around AGNs, quantify radiation near the central black hole, model radiation transfer to the host galaxy, and simulate the effects of hydrodynamics and radiative transfer on the host galaxy's energy output. Analytical methods and computational simulations were used to explore AGN behavior and its impact on the cosmic environment where the latest Python3 has used in computations and simulations. The results are well pleased with the previous theoretical works of the others and with observation under the minimal boundary conditions set.

# Acknowledgment

First and foremost, I would like to express my heartfelt gratitude to the Almighty for His divine guidance and blessings that have sustained me throughout my academic journey.I am deeply indebted to my esteemed advisor, Dr. Tolu Biressa, for his invaluable mentorship, unwavering support, and constant encouragement. His exceptional expertise and dedication have been instrumental in the successful completion of this thesis. I would also like to acknowledge the generous financial support provided by Jimma University. This support has enabled me to fully immerse myself in my research and bring this thesis to fruition. Finally, I would like to express my profound love and appreciation to my family and friends. Their unwavering support and encouragement have been an invaluable source of strength and motivation throughout my academic endeavors. To all who have contributed to this work, I extend my sincere gratitude. Your contributions have made this achievement possible.

# Chapter 1

# Introduction

## 1.1 Background and Literature Review

Active galactic nuclei(AGN) are compact cores of a special category of galaxies that are characterized by high luminosity of non-stellar origin. They emit massive amounts of energy and have a profound impact on the overall structure and behavior of the universe. These enigmatic entities are shrouded in swirling clouds of dust, making it difficult to observe their inner workings while emitting powerful radiation. The first recorded observational evidence for the existence of active galactic nuclei came from Edward A. Fath in 1908 while collecting spectra of star clusters and spiral nebulae at the Lick Observatory . Then, due to Seyfert's findings, the systematic study of galaxies with nuclear emission lines started [2]. As a result, objects that resemble them are now known as Seyfert galaxies. However, Seyfert's (1943) methodical investigation was insufficient to establish active galactic nuclei (AGN) as a prominent area of astronomy.

Additionally, one of the major efforts in comprehending AGN, including the identified active elliptical radio source galaxies like Messier 87 and Centaurus Bolton, was the advent of radio astronomy in the 1950s [3]. Based on these findings, their radio luminosities were several orders of magnitude higher than that of a typical galaxy [4]. Due to the bright emission generated at their nuclei, Seyfert galaxies, quasars, and collectively powerful radio galaxies are now collectively referred to as active galactic nuclei (AGN). Observers and theorists were forced to pay attention to these findings, and ever since, AGN have been the focus of significant research [5]. Generally speaking, the discovery of quasars in the 1960s brought attention to the topic and contributed to our current understanding of it; these objects are AGNs in galaxies [6]. It took somewhat longer for the theory to emerge that the majority of galaxies, particularly those with dynamically relaxed bulges, had inactive SMBHs in their centers [7]. According to Lynden-Bell's (1969) theory, tremendous amounts of energy could be produced on a tiny scale by matter accreting onto supermassive black holes. But in the late 1960s, it was thought that black holes might exist, and the mechanisms generating such massive amounts of energy were purely theoretical for many years [8]. Because AGN are visible at a wide range of redshifts and may be used to study the evolution of supermassive black holes, they are the primary source of information about black holes on this scale, which makes their study very significant [9, 10].

Gaining insight into the complex interaction between matter and energy in their surrounding environment is essential for discovering the secrets of their immense power and effect. Delve into the realm of radiative transfer and hydrodynamics, which are fundamental physical processes that govern the intrinsic cosmic ballet occurring around active galactic nuclei (AGNs). These processes play a crucial role in shaping the dynamic interactions and energy exchanges within this enigmatic environment [11, 12, 6]. Hydrodynamics delves into the motion of fluids, in this case, the superheated gas swirling around a black hole in an accretion disk. It governs how this gas is pulled in, flung out, and sculpted by the immense gravitational forces at play[11]. Radiative transfer is the study of how light and other types of radiation travel through the complex environment surrounding active galactic nuclei. It allows us to understand how energy is taken in, redirected, and released, providing insights into the intricate mechanisms at play within the AGN's energetic processes [12].

Comprehending the hydrodynamics and radiative transfer mechanisms surrounding AGNs is of great astrophysical importance. These mechanisms control the accretion and feedback mechanisms that dictate the development and evolution of the black hole and its host galaxy [13]. Radiation-driven winds can remove gas from the galaxy, which can quench star formation and alter galactic morphology [14]. By unraveling this cosmic ballet, we gain a better comprehension of the most energetic phenomena in the Universe and clarify the complex. Exploring the mysteries of AGNs is not just a theoretical pursuit. Understanding their dynamics will have a significant impact on how we understand the composition and evolution of the cosmos. We can follow the development of galaxies from their infancy to their mature states by studying AGNs. It sheds light on the complex interaction between radiation and gravity that controls the vast operations of the universe [11, 6].

The study of active galactic nuclei (AGNs) has been a central focus of astrophysical research for decades, with numerous studies delving into specific aspects of AGN physics. One key area of investigation has been the formation of broad emission lines in the AGN spectra. These broad lines are indicative the presence of high-velocity gas clouds in the vicinity of the central supermassive black hole. Peterson (1997) provides a comprehensive overview of the observational and theoretical aspects of broad emission line formation in AGNs, highlighting the complex interplay between the accretion disk, broad-line region, and black hole environment[15]. Despite the wealth of knowledge gained from these focused studies, a comprehensive understanding of AGN physics requires different approach theoretical models and numerical simulations. This integrated approach is essential for addressing the physical processes, feedback mechanisms, and the observed diversity of AGN properties across different cosmic environments and evolutionary stages. Motivated by this scientific necessity, we concentrate on studying hydrodynamic radiative transfer process around the AGN.

## 1.2 Statement of the problem

The hydrodynamics of radiative transfer process surrounding active galactic nuclei is a subject of strong theoretical and observational investigation, and the astrophysics of AGN is one of the long-standing issues that has been the subject of frequent searches [16]. The complex interactions between radiative transfer mechanisms and hydrodynamics in the surroundings of active galactic nuclei (AGNs) make studying them a complex task [17]. Deciphering the intricate dynamics of outflows, accretion processes, and radiation transfer around AGNs is essential to comprehend their influence on galactic evolution and the larger universe. However, there are many gaps in our current understanding due to the intricacy of these processes, which span a broad range of spatial and temporal scales. To fill in these gaps and understand the complex radiative transmission and hydrodynamics near AGNs, new mathematical and physical methods, computational simulations, and theoretical models are needed. In the end, this research attempts to close these gaps and offer a greater understanding of the physical mechanisms underlying AGN behavior.

**Research questions**

1. What is the physical processes that govern the emission and absorption of radiation around active galactic nuclei?
2. What amount of the radiation processed at the horizon of the AGN being emitted?
3. How does the radiation emitted from the AGN be transferred to the host environment?
4. In what way will the hydrodynamic radiative transfer effect is included in the energy out put of the host galaxy?

## 1.3 Objectives

### 1.3.1 General objective

To study the hydrodynamic radiative transfer process around active galactic nuclei.

### 1.3.2 Specific objectives

- To describe the physical processes that govern the emission and absorption of radiation around active galactic nuclei.

- To derive the amount of radiation processed at the horizon of the AGN being emitted
- To workout the process how the radiation emitted from the AGN is being transferred to the host galaxy
- To model the hydrodynamics radiative transfer effect in the energy out put of the host galaxy

## 1.4 Methodology

The Einstein General relativistic hydrodynamic field equations are used for both geometrical physical structure of the system and the interaction process within and the surrounding environment. The Kerr-Newmann metric is considered assuming a centrally spinning supermassive black hole in the description of the spacetime geometry. The physical processing structure of the nucleus is assumed with the thin accretion disc, that of the Shakura-Sunyaev model. The metric and the high gravity effect around the nucleus are assumed to incorporate the interaction of the system with the environment including self-interaction that determines the inflow and outflow of energy-momentum. In particular, the outflow is considered as radiation mainly sourced by the accretion disc process. The General relativistic radiative transfer equation is considered in the radiation outflow that includes the emissions and interaction with the dust environment. For numerical analysis the latest python3 is used. For document preparation Latex is used. The scheme of the thesis is organized as: chapter2 introduces the active galactic nuclei, Chapter 3 delves into the Radiation model and its effects on the environment. Chapter 4 develops the relativistic hydrodynamic equations. Chapter 5 presents the results and discussions. The final chapter, Chapter 6, offers a summary and conclusion.

## 1.5 Limitations of the study

The lack of thorough knowledge in the use of software tools needed for simulating radiative transfer processes and hydrodynamics near active galactic nuclei was the thesis's drawback. This restriction results from a lack of training resources or budgetary limitations. Furthermore, the emphasis on overcoming these obstacles can take time and funds away from carrying out in-depth studies of the particular phenomena connected to active galactic nuclei.

## 1.6 Ethical considerations

The rules and guidelines of the university were carefully followed and preserved. The ethical approval, complete with the required citations and verification, were provided by the Jimma University College of Natural Sciences Ethics Committee and Research Review.

# Chapter 2

# Active Galactic Nuclei and its Environment

Active galactic nuclei (AGN) refer to the energetic phenomena observed in the central regions of some galaxies. These phenomena cannot be attributed solely to the stellar population within the galaxy, as the nuclear regions of AGN galaxies are much brighter than can be explained by the stellar activity alone [18]. AGN are characterized by a compact, small region at the center of a galaxy that emits radiation across the entire electromagnetic spectrum, from radio to gamma-rays [18, 15]. The luminosities of active galactic nuclei can be extremely large, sometimes significantly exceeding the luminosity of the entire host galaxy [18].

Unlike the spectra of stars or normal galaxies, the spectra of AGN cannot be explained by traditional blackbody emission at a single temperature or a small range of temperatures. Instead, non-thermal processes, particularly incoherent synchrotron radiation, have been proposed as the primary mechanism behind the unique spectra of AGN [15]. This type of radiation is produced by charged particles being accelerated in a curved or spiral path in the presence of a strong magnetic field [15].

The high energy output from a small volume and the relativistic internal motions of AGNs are primarily attributed to the presence of a super-massive black hole at the center of the galaxy. AGNs are powered by accretion of matter onto a super massive black hole at the center of a galaxy. Accretion of matter on to super-massive black-hole is formed by gravitational attraction of surrounding gas, dust and stars toward the black-holes. As matter falls into the black hole, it forms an accretion disk around it. The intense gravitational forces and friction within the accretion disk generate enormous amounts of energy [18]. The relativistic speeds observed in AGNs are a result of the strong magnetic fields and the acceleration of charged particles in the vicinity of the black hole. These particles are accelerated to near the speed of light and emit radiation. Overall, the compactness, high energy output, and relativistic motions of AGNs are all consequences of the extreme physical processes occurring in the vicinity of super-massive black holes, making them some of the most fascinating and mysterious objects in the universe [18].

One of the key observational features of AGN is the presence of broad and narrow emission lines in their spectra, which are indicative of the high-velocity gas surrounding the central black hole. Many different classes of AGN are present with having different observational properties and are observed in a variety of forms, including quasars, radio galaxies, Seyfert galaxies, and blazars. But, the largest classes of AGN are seyfert galaxies and quasars. The difference between them is the amount of radiation that is emitted by the compact central source [19].

### 2.0.1 Seyfert Galaxies

The seyfert galaxies are discovered in 1943 and named after American astronomer carl seyfert. They are a type of spiral galaxy with a characteristics of extremely bright and an active central nucleus and have a broad emission lines. This broadened emission lines is due to the source of the emission moving at high speeds.On the basis of the spectrum, Seyfert galaxies are classified as type 1 or 2. In a type 1 spectrum, the broadening of the allowed lines is indicative of high-velocity gas motion, with velocities on the order of $10^4$ km/s. This suggests that the gas is moving at very high speeds. potentially due to the presence of a super-massive black hole at the center of the galaxy [20].

But, in a type 2 spectrum, all lines are narrower and more similar in width, typically with velocities less than $10^3$ km/s. This implies that the gas motion is less extreme and likely not influenced by a super-massive black hole. The narrower lines indicate lower velocities and a different physical environment within the galaxy. Transitions between these types and intermediate cases have sometimes been observed. The reason for the difference is thought to be that the allowed lines are formed in denser gas near the nucleus, and the forbidden lines in more diffuse gas further out. In type 2 Seyfert galaxies, the denser gas is missing or obscured [20].

Almost all Seyfert galaxies with known Hubble types are spirals; the possible exceptions are of type 2. They are strong infrared sources. Type 1 galaxies often show strong X-ray emission. The true Seyfert galaxies are relatively weak radio sources. However, there are compact radio galaxies with an optical spectrum that is essentially the same as for Seyfert galaxies. These should probably be classified with the Seyfert galaxies. In general, the stronger radio emission seems to come with a type 2 spectrum. It is estimated that about 1% of all bright spiral galaxies are Seyfert galaxies. The luminosities of their nuclei are about $10^{36} - 10^{38}W$, of the same order as all the rest of the galaxy. Brightness variations are common. The total energy emitted by the nuclear source at visible wavelengths is comparable to the energy emitted by all of the stars in the galaxy (i.e.,$\approx 10^{11}L_\odot$) [20].

### 2.0.2 Quasars

The 1960s marked a turning point in astronomy with the discovery of quasars. These celestial objects hold the distinction of being the most luminous and distant active galactic nuclei (AGNs) known to exist [21]. Imagine a celestial powerhouse so energetic that its central core outshines the combined light of all its constituent stars by a factor of 100. This is precisely what makes quasars stand out. Their incredible brilliance extends across the entire electromagnetic spectrum, from radio waves to X-rays, making them detectable from immense distances. This remarkable luminescence across the spectrum hints at the non-thermal processes at play within quasars. Unlike stars, which generate light through nuclear fusion, quasars unleash their energy through a different mechanism. The leading explanation for their unique spectra is incoherent synchrotron radiation. This phenomenon arises when charged particles, like electrons, are accelerated along a curved path within a strong magnetic field. As these particles gyrate, they emit electromagnetic radiation across a broad range of wavelengths, precisely aligning with the observed spectra of quasars. Understanding synchrotron radiation as the primary mechanism behind quasar emission is crucial. It plays a key role in deciphering not only the properties of quasars but also of other active galactic nuclei. By delving deeper into the intricacies of this process, astronomers can unlock the secrets of these enigmatic powerhouses and gain valuable insights into the energetic phenomena unfolding within them[15].

### 2.0.3 Radio Galaxies

Since the 1950s, astronomers have been diligently studying the shapes and sizes of the radio-emitting regions within radio galaxies [22]. This era coincided with the development of radio interferometers, instruments that achieved the remarkable feat of matching the resolution of optical telescopes. One of the most striking features revealed by these observations is the double-lobed structure that dominates many powerful radio galaxies. These lobes, which emit intense radio waves, reside on opposite sides of the central galaxy, sometimes extending to vast distances [23]. In some cases, the separation between these lobes can be as enormous as 6 megaparsecs (Mpc) – nearly ten times the staggering distance between our own Milky Way galaxy and its closest major neighbor, Andromeda [24].

The powerful radio emission from these galaxies isn't generated through the same thermal processes that govern the light we perceive from stars. Instead, it originates from a phenomenon called synchrotron radiation. This type of radiation arises when charged particles, like electrons or their antimatter counterparts (positrons), spiral or curve along a path within a strong magnetic field. As these particles accelerate along their trajectory, they release electromagnetic radiation, detectable as radio waves in the case of radio galaxies. The radio luminosity, or total power output in the radio band, of these galaxies can be truly astounding, ranging from $10^{33}$ Watts to a mind-boggling

$10^{38}$ Watts. This emission can even rival the total luminosity of an entire normal galaxy. Understanding the origin of the energetic electrons and the powerful magnetic fields that govern synchrotron radiation remains a key challenge. Additionally, pinpointing the source of the energy that these electrons utilize for their high-speed gyrations is an ongoing mystery [20].

### 2.0.4 Blazars

Blazars are a fascinating class of astronomical objects renowned for their extreme outbursts of energy [16]. They emit intense and rapidly fluctuating electromagnetic radiation across the entire spectrum, encompassing everything from radio waves to high-energy gamma rays [25]. This immense power source originates from supermassive black holes residing at the cores of galaxies. These black holes are actively accreting, or pulling in, vast quantities of surrounding matter. As this material spirals inwards towards the black hole's intense gravity, it releases tremendous energy, fueling the blazar's phenomenal luminosity. Additionally, these energetic regions around the black hole launch powerful jets of particles and radiation that can be oriented in our direction, further contributing to the blazar's brilliance. Blazars categorized into two primary groups: flat-spectrum radio quasars (FSRQs) and BL Lacertae objects (BL Lacs). The key distinction lies in the presence or absence of prominent emission lines in their spectra. FSRQs exhibit strong emission lines, indicating the existence of regions with rapidly moving, hot gas surrounding the central black hole. In contrast, BL Lacs display weak or entirely absent emission lines. This suggests that we might be observing BL Lacs from an angle less directly aligned with the jet, potentially obscuring the broad-line region from our vantage point. Therefore, the orientation of the observer relative to the blazar's jet appears to play a crucial role in how we perceive these enigmatic objects [16].

## 2.1 Structure and Composition of AGN

AGN have complex structures and compositions, including a thick, dusty torus, that obscures or hides the direct view of the accretion disk and the black-hole, and hot, ionized gas that emits radiation across the electromagnetic spectrum. Active Galactic Nuclei (AGN) are extremely luminous and compact regions at the centers of galaxies, powered by accretion onto supermassive black holes. The structure and composition of AGN are complex, and they consist of several key components [16].

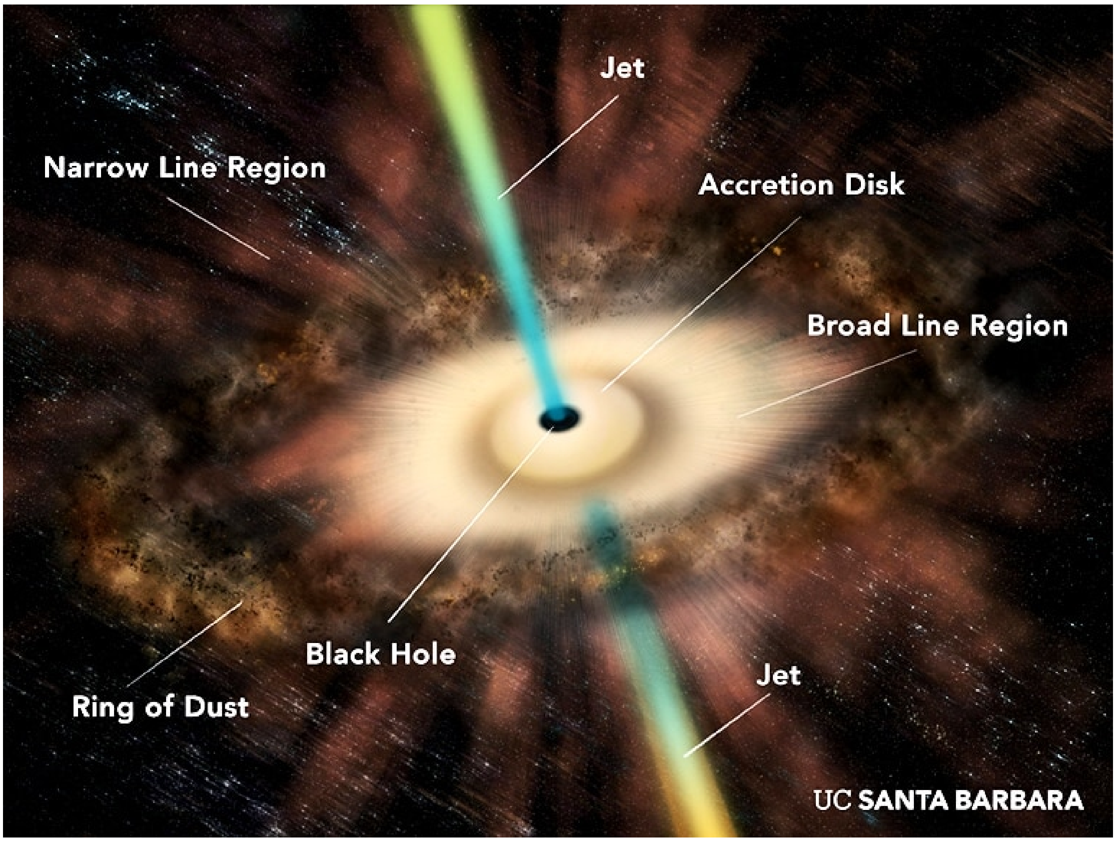


Figure 2.1: Structure of active galactic nuclei (Image Credit: Matt Perko, UCSB)).

### 2.1.1 Accretion Disk

The accretion disk, a spinning circle of gas and dust, surrounds the supermassive black hole at the heart of an Active Galactic Nucleus (AGN). This disk is essential for sustaining the enormous energy production that characterizes AGN. The disk's constituent material, mostly hydrogen gas with some dust particles, is pulled inward by the black hole's tremendous gravity from the nearby galaxy [26]. The interaction of internal pressure and gravity determines the structure of the accretion disk. The disk becomes much thinner than its width and takes on a flattened, donut-like appearance. This geometry results from a balance between the pressure that the hot gas in the disk puts forth and the gravity of the black hole pulling inward. Friction from the black hole causes the material to lose angular momentum and energy as it orbits it This energy loss forces the material to gradually spiral inwards towards the black hole, reaching ever-increasing velocities [12]. Within the accretion disk, an extreme environment is created by the close proximity to the supermassive black hole. The material falling here is accelerated to almost the speed of light by the strong gravity. This is a very effective process that transforms a large amount of the mass-energy of the material into different types of energy. The main output, which is the radiation that characterizes AGN, is powerful electromagnetic radiation spanning the spectrum from radio waves to X-rays [27].

### 2.1.2 Broad-Line Region (BLR)

Broad emission lines are one of the dominant features of many AGN spectra. The broad-line region (BLR) plays a particularly important role in our understanding of AGNs by virtue of its proximity to the central source. The BLR potentially can provide a useful probe of the central source for at least two reasons. First, the bulk motions in the BLR are almost certainly determined by the central source, with gravity and radiation pressure competing. Second, the BLR reprocesses energy emitted by the continuum source at ionizing ultraviolet energies that cannot be observed directly, and thus the emission lines provide indirect information about this important part of the continuum [15].

The BLR is a region of highly ionized gas located close to the central black hole. It emits broad emission lines in its spectrum, which are produced by the interaction of the intense radiation from the accretion disk with the surrounding gas. The BLR provides important clues about the physical conditions and dynamics near the black hole [15].

### 2.1.3 Narrow-Line Region (NLR)

The NLR is a more extended region of ionized gas located further out than the BLR encircling the center black hole. Its spectra is characterized by thin emission lines that are caused by lower density gas that has been ionized by radiation from the accretion disk and other sources. There are at least three interconnected reasons why the NLR in AGNs is interesting. First off, the NLR is the largest spatial scale where at which the central source's ionizing radiation predominates over that of other sources. Secondly, the NLR is the sole component of AGN that can be spatially resolved in the optical; this is significant since the central source clearly illuminates the NLR in a non-isotropic way [15].

### 2.1.4 Dust Torus

Active galactic nuclei (AGNs) are incredibly luminous objects powered by supermassive black holes at their centers. Surrounding these central regions lies a donut-shaped structure called the dust torus, composed of dust and gas. This dust torus plays a critical role in how we observe AGNs. The dust torus absorbs a significant portion of the radiation emitted by the hot, swirling accretion disk surrounding the black hole [28]. This accretion disk is where most of the AGN's energy originates. The absorbed radiation is then re-emitted by the dust at longer wavelengths, primarily in the infrared range. The orientation of the dust torus relative to our line of sight can significantly impact our observations of the AGN. Imagine looking through a doughnut head-on versus looking down its central hole. When the dust torus is viewed edge-on, we have a relatively clear view of the central regions and the hot accretion disk. This allows us to directly observe the intense ultraviolet and X-ray radiation emitted from the disk. These AGNs are classified as "unobscured." Conversely, if the dust torus is viewed face-on, our line of sight is blocked by the bulk of the dust. This significantly obscures the central regions and the hot accretion disk. We primarily observe the re-radiated infrared emission from the dust itself. These AGNs are classified as "obscured" [28].

### 2.1.5 Jets

Some AGN exhibit powerful jets of charged particles that are accelerated to nearly the speed of light by magnetic fields near the black hole. These jets can extend over large distances and interact with the surrounding interstellar medium, producing lobes of radio emission. The composition of these structures includes a variety of elements and molecules, such as hydrogen, helium, oxygen, nitrogen, carbon, and various dust grains. The physical conditions within these regions, including temperature, density, and radiation field, are determined by the complex interplay of processes such as accretion, radiation transfer, and interactions with magnetic fields and surrounding gas. Understanding the structure and composition of AGN is essential for unraveling their energetic phenomena and their impact on galaxy [29].

## 2.2 Unified Model of AGN

The diversity of AGN types, as discussed in the above sections, can be attributed to the orientation of the system relative to the observer, rather than fundamental differences in the underlying physical processes, as suggested by the unified model of AGN [16]. The unifying model postulates the presence of a single underlying physical entity in order to explain the numerous properties displayed by different types of active galactic nuclei (AGN). A large portion of the morphological elements of unified models research involves investigating correlations between observed parameters. Generally, these studies are motivated by broad ideas about possible physical mechanisms involved. There is general agreement that although AGN's reported features vary widely, their fueling mechanisms are essentially similar [28].

Antonucci (1993) devised the current model for combining several forms of active galactic nuclei (AGN), and Urry and Padovani (1995) refined it. AGN were first divided into two primary categories by Antonucci's model: radio quiet and radio loud. Seyfert galaxies and radio-quiet quasars are members of the radio-quiet group; radio galaxies, radio-loud quasars, and BL Lac objects are members of the radio-loud group. The

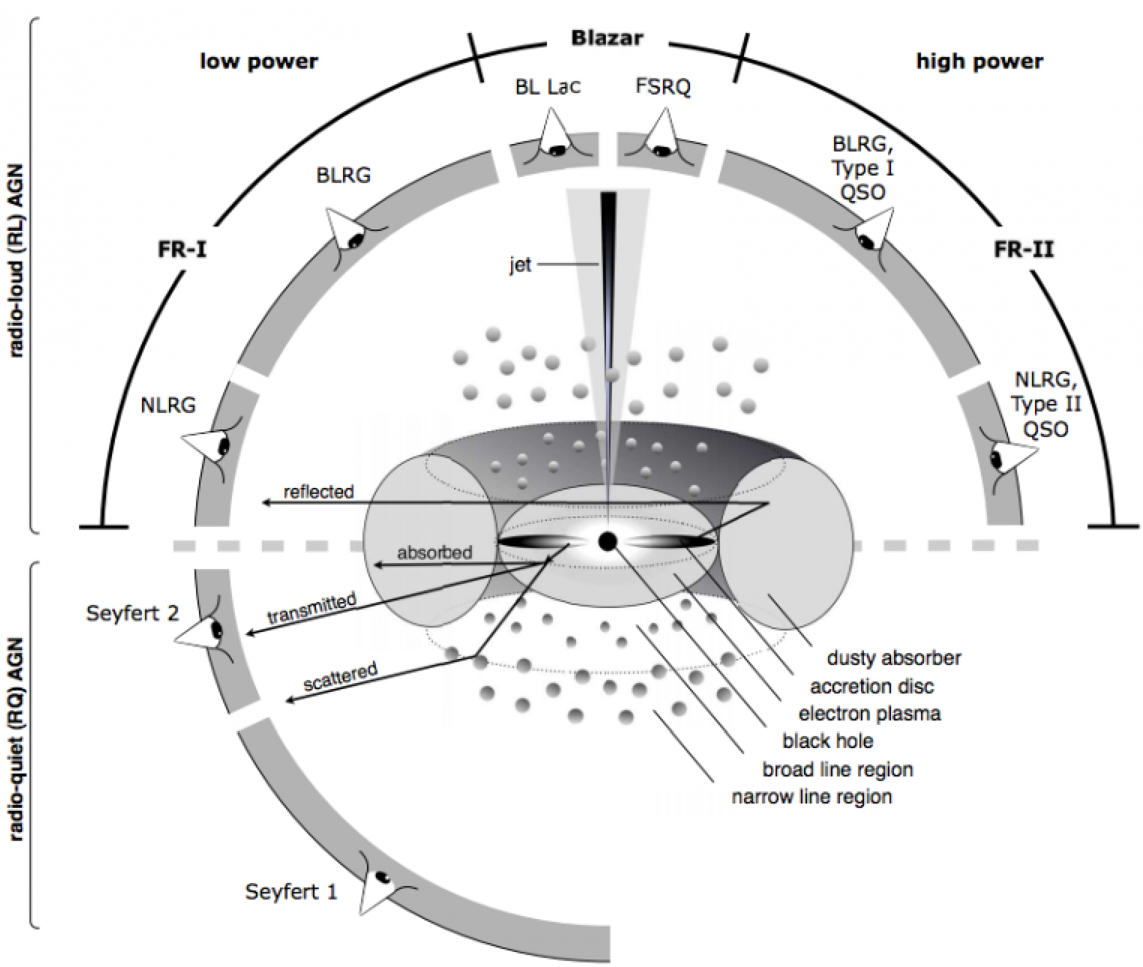


Figure 2.2: Schematic representation of the unified AGN model (Credit: Beckmann & Shrader 2012) [1]

variability properties of radio-loud and radio-quiet active galactic nuclei (AGN) differ, indicating that radio-loud AGN variability is mostly attributed to relativistic jet emission. Based on their radio luminosity, these radio-loud AGN are further divided into two different types: low-luminosity sources, like BL, and high-luminosity sources, including radio-loud quasars and FR II radio galaxies [28]. This classification is important for understanding the underlying physical processes in different types of AGN [15].

Based on their physical properties, three different types of active galactic nuclei (AGN) are distinguished in this classification. The variations in the perspectives from which we view each form of AGN are responsible for their peculiarities. As per the unified paradigm put forth by Urry and Padovani (1995) and Antonucci (1993), supermassive black holes (SMBH) are thought to be situated at the center of galaxies. Furthermore, a torus-a structure resembling a doughnut-is positioned in relation to the accretion disk and partially obstructs disk emission [28]. As a result, the observer's perspective affects how the AGN's center region appears. The unified model proposes that the innermost bright area of the AGN is surrounded by a dense belt of matter that blocks it from direct view when observed close to the equatorial plane. In essence, the differences in appearance and behavior of AGN are primarily due to our viewing angle relative to their orientation in space [28].

Objects like Seyferts, LINERs, BL Lac objects, Optically Violent Variable objects (OVV), Blazars, and broad-line radio galaxies are all included in the AGN class. As previously said, these items share fundamental traits in common. This indicates that even if they differ, they have some important characteristics in common that make them belong to the AGN class [28]. The angle at which active galactic nuclei (AGN) are seen affects how they appear. Optical observations of type-I AGNs reveal them as unique, point-like objects that emit a great deal more light than the nearby stars in their home galaxy. Their spectral energy distribution (SED) and lack of significant stellar absorption lines indicate this non-stellar origin. Type-II AGNs, on the other hand, do not show this excess emission. Furthermore, there can be large variations, possibly by several orders of magnitude, in the non-stellar nuclear source's relative brightness with respect to the host galaxy's overall luminosity. This difference in appearance, which results from the AGN's direction with regard to the viewer, offers crucial information about the nature and behavior of these objects [30].

Within the immediate cosmos, The brightness of active galactic nuclei (AGNs) can be dominated by starlight, with many AGNs being far fainter than the galaxies they host. A high stellar-mass AGN host, for example, can have a V-band brightness of up to $10^{44} ergs^{-1}$, which is significantly more than the luminosity of many nearby type-I AGNs. When studying AGN spectra produced with large entrance aperture instruments, this is a crucial factor to take into account. With decreasing wavelength, the AGN's relative brightness rises, and at UV wavelengths, starlight contamination is less of an issue [30].

Seyfert galaxies and quasars are the two main subclasses of AGNs; the distinction between them is somewhat arbitrary, but the main difference is the amount of radiation emitted by the compact central source: in a typical Seyfert galaxy, the total energy emitted at visible wavelengths by the nuclear source is comparable to the total energy emitted by all the stars in the galaxy; in a typical quasar, on the other hand, the nuclear source is more than 100 times brighter than the galaxy's stars combined. Because Seyfert galaxies and quasars were first detected using separate techniques, which led to a notable discrepancy in their luminosities, it was previously unknown that they are most likely related. The difference in brightness between the two kinds of items made it difficult to discern any possible relationship between them [31].

# Chapter 3

# AGN Radiation Model and Its Effects on Its Environment

## 3.1 Accretion process

Accretion occurs when matter falls towards an object's gravitational field, releasing energy in the process. This process generates radiant energy in various astrophysical sources, including stellar binaries, active galactic nuclei, and some types of gamma-ray bursts. Accretion has significant consequences. It results from matter in a host galaxy losing angular momentum and falling towards a supermassive black hole (SMBH). This gravitational energy is converted into heat and light, producing objects with varying luminosities and variability. Accretion and mergers are both believed to contribute to black hole growth, but accretion may play a more dominant role [32].

In active galaxies, the nucleus contains a SMBH. The activity level of the nucleus depends on the amount of matter flowing onto the black hole. As the matter falls inward, it loses energy and angular momentum. The emission of matter from near the black hole provides insights into this unresolved region[32]. Active galactic nuclei (AGN) derive their immense power from the process of matter accretion onto supermassive black holes located at the centers of their host galaxies. This accretion mechanism liberates gravitational energy, which serves as a significant source of radiation in the field of astrophysics.

Viscous dissipation occurs when matter descends inward through the swirling accretion disk, encountering friction and turbulence along its path. This dynamic interaction generates substantial heat within the gas, leading to the emission of an extensive range of radiation across the electromagnetic spectrum. Viscous dissipation represents the primary contributor to the luminosity observed in AGN, as it accounts for the energy released during this process.

The rate of viscous dissipation is given by [33]

$$E_{\text{visc}} = \frac{1}{2}\left(\frac{Mc^2a^2}{R_{\text{in}}^2}\right) \tag{3.1}$$

Where:

$E_{\textbf{visc}}$ represents the energy resulting from viscous dissipation, measured in erg/s.

$M$ corresponds to the mass of the black hole, expressed in kilograms.

$c$ denotes the speed of light, in meters per second.

$a$ signifies the black hole spin parameter, which is dimensionless and typically ranges from 0 to 1.

$R_{\textbf{in}}$ represents the inner radius of the accretion disk, measured in meters.

This equation (3.1) describes the energy released due to viscous dissipation within the accretion disk surrounding a rotating black hole. The viscous energy, $E_{\text{visc}}$, is proportional to the square of the black hole's spin parameter, $a$, and inversely proportional to the square of the inner radius of the accretion disk, $R_{\text{in}}$. The black hole's mass, $M$, and the speed of light, $c$, are also included in the expression.

The equation emphasizes how factors such as the black hole's mass, spin, and the inner radius of the disk influence the rate at which energy is released through viscous dissipation. A higher black hole spin parameter, $a$, and a smaller inner accretion disk radius, $R_{\text{in}}$, will result in a greater amount of viscous energy, $E_{\text{visc}}$, being released. This highlights the importance of these key parameters in understanding the energetics of accretion disks around rotating black holes. The accretion process depends on the geometry of the system and can occur in different ways. Spherical and non-spherical systems behave differently. Gas that accretes onto a black hole typically forms an accretion disk. However, there have been studies of spherical or quasi-spherical accretion flows onto black holes.

Two important quantities related to accretion are the Eddington luminosity and the Eddington accretion rate. The structure of the accretion disk depends on various factors, including the magnetic field strength, accretion rate, and the presence of a disk corona or jets [34]. The luminosity of the source is defined by the rate at which mass is accreted and converted to energy. The standard physical model of an AGN that starts with a central BH and is growing via mass accretion luminosity is given by

$$L_{acc} = \eta \dot{M} c^2 \tag{3.2}$$

where $\eta$ is the mass-energy efficiency conversion (typically estimated to be ≈ 0.1, but is dependent on the spin of the BH with an expected range of $\eta = 0.05 - 0.42$, and $\dot{M}$ is the mass accretion rate. The mass-energy conversion efficiency depends on the spin of the black hole, whereby high spin leads to higher efficiencies. A theoretical upper limit on $L_{acc}$ can be calculated assuming accretion of fully ionized hydrogen onto a BH of mass MBH, when the force of gravity is equal to the radiation pressure from the accretion luminosity. This upper-limit is called the Eddington luminosity and has the value

$$L_{Edd} = \frac{4\pi G M_{bh} m_p c}{\sigma_T} \tag{3.3}$$

$$L \approx 1.3 \times 10^{38} \left( \frac{M_{bh}}{M_\odot} \right) ergs^{-1} \tag{3.4}$$

where $m_p$ is the proton mass, c is the speed of light, G is the gravitational constant and $\sigma_T$ is the Thomson cross-section for an electron. It is the maximum luminosity allowed for objects that are by steady state accretion. The ratio of the observed accretion luminosity to the Eddington luminosity (called the Eddington ratio;$\lambda_{Edd}$)is a useful measure for comparing BH accretion rates over a wide range of BH masses

$$\lambda_{Edd} = \frac{L_{acc}}{L_{Edd}} \tag{3.5}$$

The term high-accretion rate AGN is often used to refer to sources with high values of $\lambda_{Edd}$ (i.e., $\lambda Edd \geq 0.1$). The value of $L_{acc}$ used in Equation(3.5) is assumed to be the radiative bolometric output of the AGN [35].

## 3.2 Radiation model

Examining a variety of physical processes is necessary to understand the mechanics behind AGN radiation. The tremendous energy output is produced by emission processes, such as synchrotron radiation from jets and thermal radiation from the accretion disk. But a whole image requires taking collimation into account, which concentrates radiation into strong jets. Furthermore, emission lines offer important insights into the composition and flow of the gas surrounding the black hole. Lastly, another shaping of the observed spectrum may come from dust and gas in the AGN and its surroundings absorbing and scattering radiation.

### 3.2.1 Emission

Active galactic nuclei (AGN), the incredibly energetic hearts of some galaxies, baffle astronomers with their immense brightness. These compact regions outshine the billions of stars in their host galaxies, emitting across the entire electromagnetic spectrum, from radio waves to gamma rays. This mysterious phenomenon is thought to be powered by supermassive black holes at the galactic center [36]. The leading theory suggests that the tremendous energy output is due to the swirling accretion disk of gas and dust surrounding the supermassive black hole. As this material spirals inwards, it heats up to unimaginable temperatures, releasing tremendous amounts of light in the process. Additionally, the immense gravitational pull of the black hole accelerates some of this infalling matter to near light-speed, generating powerful jets that shoot out perpendicular to the accretion disk. These jets can extend far beyond the galaxy itself, further contributing to the overall energy output [37].

The specific characteristics of the emitted radiation depend on several factors. The mass of the black hole, the rate at which it devours material, and the orientation of the accretion disk all influence the observed spectrum. For instance, if our line of sight coincides with a jet, the emission will be significantly boosted in that direction, creating a class of AGN known as blazars [38]. Additionally, dust and gas surrounding the black hole can absorb some of the radiation, leading to variations in the observed spectrum across different AGN types.

### Thermal Disk Emission

Within the grand spectacle of active galactic nuclei (AGN) lies a crucial component – thermal disk emission. This refers to the light radiating from the swirling accretion disk of gas and dust encircling the supermassive black hole at the AGN's heart. Understanding this thermal emission provides key insights into the energetic processes at play [39]. The immense gravitational pull of the black hole accelerates the infalling material in the accretion disk. Friction between gas particles within the disk causes them to heat up to millions of degrees. This scorching gas radiates intensely across a broad range of wavelengths, peaking in the ultraviolet and optical regions of the electromagnetic spectrum. The spectrum follows a pattern characteristic of a hot, glowing object called a blackbody [40].

As approximation, the blackbody radiation is given by [15]

$$B_\nu = \frac{2h\nu^3}{c^2}\left(\frac{1}{e^{h\nu/\kappa T(r)} - 1}\right) \tag{3.6}$$

Where T(r) is the disk temperature at radius r from the center, which is given by

$$T(r) \approx T\left(\frac{Rs}{r}\right)^{1/2} \tag{3.7}$$

and the density of the disk is given by [33]:

$$\rho(r) \approx \rho\left(\frac{Rs}{r}\right)^{3/2} \tag{3.8}$$

The flux emitted per unit area is $F_\nu = \pi B_\nu$ and the disk is assumed as geometrically thin ( though optically thick ) and has radial symmetry so that a ring of width dr at radius r will have a specific luminosity

$$dL_\nu(r) = 2\pi r \cos i \pi B_\nu dr \tag{3.9}$$

Where i is the inclination of the disk to the plane of the sky. The total specific luminosity of the disk is given by integrating over full range of radii:

$$L_\nu = \frac{4\pi^2 h\nu^3 \cos i}{c^2}\int_{R_{in}}^{R_{out}} \frac{r dr}{e^{h\nu/\kappa T(r)} - 1} \tag{3.10}$$

Where

$R_{in}$ is inner boundary of the disk

$R_{out}$ is outer boundary of the disk

However, the intense gravity and extreme environment of the accretion disk introduce complexities. Relativistic effects, where particles move at speeds close to the speed of light, become significant. Light emitted from the inner, hotter regions of the disk experiences a gravitational redshift – its wavelength stretches, shifting the peak of the thermal emission towards longer wavelengths, like the infrared or even the radio regime [41]. The phenomenon known as Bremsstrahlung, or "braking radiation" in German, is one of the main factors causing the X-ray emission from AGNs. High-energy electrons in the heated gas lose some of their kinetic energy and release X-ray radiation when they hit with atomic nuclei. This ongoing process produces a wide range of X-ray radiation, which offers important information on the density and temperature of the electrons as well as other physical parameters within the accretion disk [42]. Recombination is another important mechanism of emission. Ionized atoms can undergo an energy transition to a lower level when free electrons in the heated gas come into contact with them and take an electron from them. The caught electron releases energy during this process as radiation at a particular frequency specific to the concerned element. Astronomers can determine the elements included in the gas within the accretion disk by examining the detected recombination lines in the AGN spectrum. This helps to clarify the chemical makeup of this heated and turbulent environment [10].

### Synchrotron Radiation

AGN spectra cannot be described in terms of blackbody emission at a single temperature, or as a composite over a small range in temperature. Non-thermal processes, primarily incoherent synchrotron radiation, were thus invoked early on to explain quasar spectra. In general, the broad-band SED of a quasar continuum can be characterized crudely as a power law [15]

$$F_\nu = C\nu^{-\alpha} \tag{3.11}$$

Where $\alpha$ is the power-law index, C is a constant and $F_\nu$ is the specific flux usually measured in units of $ergs^{-1}cm^{-2}Hz^{-1}$.

Synchrotron radiation is a key contributor to the electromagnetic emissions observed in active galactic nuclei (AGN). It arises from the interaction between high-energy electrons and a strong magnetic field. Within the energetic environment of AGN, particularly in radio-loud varieties, synchrotron radiation plays a crucial role in understanding the particle acceleration mechanisms and the formation of powerful jets. The production of synchrotron radiation in AGN hinges on two key ingredients: highly energetic electrons and a strong magnetic field. The supermassive black hole at the heart of an AGN is believed to be the driving force behind particle acceleration. As matter falls into the black hole's accretion disk, it experiences powerful magnetic fields and intense gravitational forces. These extreme conditions can accelerate electrons to near the speed of light, imbuing them with tremendous energy. Additionally, the accretion disk itself and the environment surrounding the black hole are thought to harbor strong magnetic fields, providing the stage for synchrotron emission [43].

When a high-energy electron encounters a strong magnetic field, its path is no longer a straight line. Instead, the electron gets deflected and forced into a helical trajectory, spiraling around the magnetic field lines. This spiraling motion is a form of acceleration, and according to the laws of electromagnetism, an accelerating charged particle emits radiation. In the case of synchrotron radiation, the emitted radiation spans a broad range of the electromagnetic spectrum, from radio waves to X-rays, depending on the energy of the electrons and the strength of the magnetic field [42].

### 3.2.2 Emission Lines

Active galactic nuclei (AGN) emit not only a continuous spectrum of light but also specific wavelengths of light known as emission lines. These lines act like fingerprints, revealing the composition and conditions of the gas surrounding the supermassive black hole at the AGN's center [10]. Emission lines arise when high-energy radiation from the hot accretion disk interacts with nearby gas clouds. This radiation excites the atoms in the gas, causing them to jump to higher energy levels. However, these excited states are unstable, and the atoms quickly return to their ground states, releasing the excess energy as light at specific wavelengths. The specific wavelengths emitted depend on the elements present in the gas and the amount of energy absorbed [44].

Scientists categorize emission lines in AGN spectra into two main types: narrow and broad. Narrow emission lines originate from gas clouds farther from the black hole, where velocities are relatively low. These lines provide information about the composition and motion of gas in the broader galactic environment surrounding the AGN [15]. Broad emission lines, on the other hand, offer a closer look at the region directly around the black hole. Their widths indicate extremely high gas velocities, exceeding thousands of kilometers per second. This suggests a region very close to the black hole, likely within the broad-line region (BLR) – a zone of hot, fast-moving gas swirling around the black hole. By analyzing these broad lines in detail, astronomers can probe the dynamics and geometry of the BLR, gaining insights into the black hole's spin and the influence of its immense gravity [45].

### 3.2.3 Collimation

Active galactic nuclei (AGN) are renowned for their immense luminosity, but a surprising aspect of this emission is its focus. Instead of radiating uniformly in all directions, AGN often display powerful jets that shoot out perpendicular to the accretion disk, channeling energy and matter far beyond the confines of the host galaxy. This phenomenon is known as collimation, and understanding its mechanism remains an active area of research [46]. The leading theory for collimation centers around the interplay between the supermassive black hole at the AGN's core and its swirling accretion disk. Magnetic fields are believed to play a crucial role. As the hot, ionized gas in the disk rotates, it becomes entangled with these magnetic field lines. These field lines are then dragged inwards towards the black hole, forming a powerful funnel-like structure known as the magnetosphere [47].

Within the magnetosphere, the intense magnetic fields accelerate a small fraction of the infalling gas to near light-speed. This highly energetic and collimated outflow escapes the black hole's pull along the polar axis, forming the jets. The specific details of how this acceleration occurs remain a subject of debate, with various mechanisms like magnetohydrodynamic (MHD) processes and centrifugal forces being explored [48].

The collimation process is not perfect. Observations reveal jets with varying degrees of collimation, some appearing well-defined and narrow, while others exhibit wider, more turbulent structures. This suggests that the collimation process might be influenced by various factors, including the black hole's spin, the properties of the accretion disk, and the presence of a surrounding dusty torus [49].

### 3.2.4 Absorption and Scattering

Active galactic nuclei (AGN) are brilliant beacons, but their emitted light can be significantly affected by the material surrounding them. Absorption and scattering can alter the observed spectrum, offering valuable insights into the environment obscuring the central engine [50].

Photoelectric absorption is one important type of absorption. High-energy photons, which are usually X-rays or ultraviolet light, can absorb fully when they come into contact with gas atoms. That energy from the absorbed photon is not lost, though. It is employed to expel an electron from the atom, which may affect the spectrum that is seen and may heat the gas [42].

Bound-bound absorption is another important mode of absorption. Here, atoms interact with photons of particular energies, which causes the electrons in those atoms to leap to higher energy levels. The energy difference between the starting and final states of the electron and the absorbed energy are exactly equal. Absorption lines in the AGN spectrum are a sign of this process and provide important information about the gas's constituent composition [10].

And lastly, free-free absorption. This process bears some similarities to bremsstrahlung. A portion of a photon's energy can be absorbed by high-energy electrons in the heated gas as they contact with atomic nuclei. On the other hand, the photon is not totally consumed, unlike photoelectric absorption. Rather, the electron absorbs the energy and keeps going, whereas the photon may get scattered or take a slightly different route. The overall opacity of the medium is influenced by free-free absorption, which impacts the radiation propagation efficiency within the AGN environment [42].

The strength and location of absorption lines depend on the abundance of specific elements and the physical conditions within the absorbing gas. Astronomers can use these features to identify different gas phases, like cold, neutral gas or hot, ionized gas, along the line of sight to the AGN [51]. Additionally, the analysis of absorption lines can reveal the velocity of the absorbing gas, providing clues about its motion and potential interaction with the AGN's outflowing jets [52]. Scattering, on the other hand, doesn't destroy light; it simply changes its direction. When a photon interacts with an electron in an atom or molecule, it can be deflected off course without losing any energy. This process can be further categorized as electron scattering, where the photon interacts with a free electron, or Rayleigh scattering, where the photon interacts with a bound electron. Both types of scattering can cause the observed spectrum of the AGN to be smeared or reddened, as the originally emitted photons are redirected along slightly different paths [53].

The presence and strength of scattering can be indicative of the dust distribution around the AGN. By studying the reddening of the spectrum, astronomers can estimate the amount of dust obscuring the central engine. Additionally, detailed analysis of the scattered light can reveal the geometry of the dusty region, providing clues about the presence of a dusty torus – a doughnut-shaped structure surrounding some AGN that can significantly obscure the direct view of the central engine [54].
In the dynamical simulations, AGN radiation is emitted anisotropically, following

$$F(r,\phi) = \frac{L}{4\pi r^2} f(\phi) \tag{3.12}$$

Where L is the luminosity of the AGN, r is the distance from the AGN, $\phi$ is the angle from the equitorial axis of the AGN, and the anisotropy function $f(\phi)$ is defined to be

$$f(\phi) = \frac{1 + a\sin\phi + 2a\sin^2\phi}{1 + 2a/3} \tag{3.13}$$

Where $a = \left(\frac{\eta_a - 1}{3}\right)$ and $\eta_a$ is anisotropy factor , equal to the polar flux and equitorial flux. This is a free parameter to control the relative strengths of disk emission and isotropic emission.

### 3.2.5 Re-emission

Active galactic nuclei (AGN) are powerhouses of electromagnetic radiation. However, the observed light we detect isn't always a direct product of the central engine. A significant portion of the emitted light can be reprocessed and re-emitted by the surrounding material, leading to a phenomenon known as re-emission. Understanding this process offers valuable insights into the environment around the AGN and the nature of the obscuring material [55]. Thermal re-emission and dust re-emission are two primary mechanisms for re-emission in AGN. Thermal re-emission occurs when high-energy photons from the AGN interact with surrounding gas clouds. These photons can heat the gas, causing it to emit its own thermal radiation at longer wavelengths, typically in the infrared and sub-millimeter regimes. The observed spectrum of this re-emitted radiation depends on the temperature and density of the gas clouds[56].

Dust plays a crucial role in another form of re-emission. When ultraviolet (UV) photons from the AGN collide with dust grains, they can be absorbed. However, the dust doesn't simply "trap" this energy. Instead, the dust grains heat up and subsequently re-emit the absorbed energy at longer wavelengths, primarily in the infrared and millimeter regimes. This re-emission by dust can significantly redden the overall spectrum of the AGN, obscuring the view of the central engine and potentially leading to underestimates of the true luminosity [57]. The characteristics of the re-emitted radiation hold valuable clues about the environment surrounding the AGN. By studying the strength and distribution of the infrared emission, astronomers can map the distribution of dust and gas clouds around the central engine. Additionally, the analysis of spectral features arising from the re-emitted radiation can reveal the composition and physical conditions within these clouds [58]. Furthermore, re-emission can be used to probe the geometry of the obscuring material. In some cases, the re-emitted light may be delayed compared to the direct emission from the AGN. This time delay can be used to map the size and structure of the obscuring region, potentially revealing the presence of a dusty torus surrounding the central engine [55].

## 3.3 Radiation and the Dusty Torus

The total energy emitted by the AGN is its luminosity, often denoted by L. This luminosity originates primarily from the hot accretion disk surrounding the black hole. The dusty torus absorbs a fraction of the radiation emitted by the accretion disk. This fraction can be represented by the absorption coefficient ($\kappa$) and the column density ($\Sigma$) of dust along the line of sight [28]:

$$A = \kappa\Sigma \tag{3.14}$$

A: Absorption fraction (0 to 1)

$\kappa$ : Absorption coefficient (depends on dust properties and radiation wavelength)

$\Sigma$: Column density of dust (amount of dust per unit area)

The re-emission efficiency can be represented by another coefficient ($\epsilon$) [28].

$$R = A\epsilon L_{\lambda} \tag{3.15}$$

R : Re-emitted radiation

$\epsilon$ : Re-emission efficiency (depends on dust properties)

$L_{\lambda}$: Luminosity of the emitted radiation at a specific wavelength ($\lambda$)

## 3.4 AGN Effects on its Environment

### 3.4.1 Suppressive Effects

The dense environments of galaxy clusters can significantly suppress the presence of active galactic nuclei (AGNs) within their host galaxies. This is primarily due to the process of ram-pressure stripping, where the galaxies constantly interact with the hot, diffuse gas permeating the space between them, known as the intracluster medium. This

interaction can effectively remove a galaxy's cold gas reservoirs, which are essential for fueling both star formation and feeding the central supermassive black hole. Without this necessary gas supply, the black hole becomes starved and less active, leading to a suppression of AGN activity within the cluster galaxies. The dense cluster environment, through this gas stripping mechanism, can effectively shut down or drastically reduce the signatures of AGN behavior in its host galaxies.
The second factor is the reduced rate of galaxy-galaxy interactions. Compared to the field region, galaxies within clusters experience fewer close encounters with their neighbors. As a result, processes triggered by mergers or tidal interactions, which can funnel gas toward the central regions of galaxies and potentially ignite or enhance AGN activity, occur less frequently in clusters [59]. The reduced interaction rate in cluster environments translates to a lack of triggers for AGN outbursts.

### 3.4.2 Triggering Effects

Galaxies in dense environments such as clusters or groups can undergo gas loss through interactions with neighboring galaxies or the intracluster medium, a process known as ram-pressure stripping. This gas removal depletes the gas reservoir necessary for star formation and black hole feeding, potentially leading to the suppression of AGN activity. In situations where interactions with the surrounding gas environment occur, however, the effects can be quite different. Gravitational interactions with neighboring galaxies or gas inflow from cosmic filaments can channel gas toward a galaxy's core. This influx of gas can accelerate the accretion rate onto the central supermassive black hole, potentially triggering or enhancing AGN activity. The consequence is a more active black hole capable of producing powerful outflows, jets, and intense radiation spanning the electromagnetic spectrum [60].

Close encounters between galaxies play a significant role in impacting the gas dynamics of interacting systems. These encounters can funnel gas toward the central regions, ultimately activating AGNs. This process is crucial for the evolution of galaxies and the co-evolution of supermassive black holes with their host galaxies. As galaxies approach one another, their mutual gravitational pull generates tidal forces that distort their shapes. Such interactions can cause gas rearrangements within each galaxy and facilitate the transfer of gas between them. Consequently, gas can be directed toward the central regions of the galaxies during these interactions. When gas begins to flow toward the central black hole, AGN activity can be ignited. The increased accretion rate onto the black hole results in powerful radiation emission across various wavelengths, including X-ray, ultraviolet, optical, and infrared. This radiation, in turn, can influence star formation and the interstellar medium within the host galaxy, while also driving robust outflows and jets [61].

Interactions between galaxies and their surroundings can stimulate enhanced star formation within the galaxies. This increased star formation can provide more fuel for the supermassive black hole at the galaxy's center, potentially leading to more active AGNs. Tidal interactions and gravitational forces during interactions with the environment or other galaxies can disrupt and compress the gas within galaxies. Consequently, gas density in specific regions of the galaxies can increase. The heightened gas density can trigger the formation of new stars within these regions. As gas becomes denser and more concentrated, it can collapse under its own gravity, initiating star formation. This process often results in the formation of young, massive stars, particularly in areas where gas has been gathered or channeled through interactions[62].

### 3.4.3 Environmental dependence

The influence of the surrounding environment on the activity of active galactic nuclei (AGN) varies throughout galaxies and is dependent on a number of variables, including black hole properties, galaxy mass, and stellar age. Recent research has shown that environmental processes can significantly affect low-mass galaxies' gas reservoirs and the accretion onto the core black hole, making the environment a particularly important factor in these systems.The mass of a galaxy plays a crucial role in determining how its environment affects AGN activity. Low-mass galaxies, which have lower gravitational potential wells, are more susceptible to environmental influences. The interactions with neighboring galaxies, as well as the effects of the larger-scale cosmic environment, can have a more pronounced impact on the gas dynamics and star formation processes within low-mass galaxies [63].

The sensitivity of AGN activity to external causes is also influenced by the age of the star population within a galaxy. Low-mass galaxies frequently have younger stellar populations, and because of their continuous star formation and less stable gravitational conditions, their gas reservoirs may be more easily impacted by environmental events. Complex interactions can occur between the parameters of the central supermassive black hole, such as its mass and accretion rate, and the surrounding environment. Environmental activities have the potential to modify gas reservoirs and affect accretion onto black holes in low-mass galaxies. Depending on the unique properties of the black hole and how it interacts with the surroundings, this may result in variances in AGN activity [63].

### 3.4.4 AGN feedback

There is a strong connection between the formation of galaxies and the growth of super-massive black holes at their centers. The mass of the black hole is related to the mass and velocity dispersion of the bulge(center) of the galaxy. Mass of the bulge is related to the amount of stars and other matter concentrated in this central region, while the velocity dispersion refers to the range of velocities at which these stars are moving. It appears that the black hole and bulge of the galaxy grow in coordination until the activity of black hole, known as an active galactic nucleus (AGN), becomes powerful enough to produce strong radiation pressure. This radiation pressure then drives winds that expel cold gas from the intergalactic medium, ultimately halting the formation of new stars in the galaxy. This is AGN feedback, in the form of radiative pressure. This self-regulating process which links the energy released by the AGN to the surrounding gaseous medium and in this way, impacting on the evolution of the host galaxy [64, 65]. The feedback from AGN activity can also affect the distribution and properties of the gas in the intergalactic medium, impacting the formation of new galaxies and influencing the overall structure of the universe. This feedback can also play a role in regulating the growth of massive galaxies and clusters, as well as in shaping the large-scale distribution of matter.

# Chapter 4

# Relativistic Hydrodynamic Radiative Transfer Equations

## 4.1 General Relativity and Exact Solutions to Einstein Field Equations

Modern physics is changing as a result of Albert Einstein's revolutionary theory of general relativity. A significant relationship between space, time, and gravitation is established by this theory. Einstein's 1915 theory of general relativity offers a geometric explanation of gravity. It asserts that spacetime's curvature, which is brought about by the presence of mass and energy, is what causes gravity, not any conventional force. The path taken by objects traveling through spacetime is determined by this curvature. The ten complex nonlinear partial differential equations known as the Einstein field equations form the basis of the theory. They define the relationship between the distribution of matter and energy, symbolized by the stress-energy tensor, and the geometry of spacetime, represented by the metric tensor [66].

The quest for exact solutions to the Einstein field equations presents a formidable challenge owing to their intricate and nonlinear characteristics. These solutions offer a detailed description of spacetime geometry without the need for oversimplification. Nevertheless, they frequently depict idealized scenarios characterized by particular symmetries, such as a flawlessly spherical mass distribution [67].

The study of exact solutions to Einstein's field equations provides a thorough understanding of the various solutions that are accessible for sources such as vacuum, Einstein-Maxwell, pure radiation, and ideal fluid. The first part of this trip covers an overview of differential and Riemannian geometry principles as well as the methods used to find, identify, or produce these solutions. Following that, the solutions are examined with respect to their symmetry group, algebraic structure, or other invariant qualities such as certain subspaces, tensor fields, and embedding properties. Specifically, representing relativistic astrophysical entities relies heavily on accurate solutions of the Einstein-Maxwell field equations. These models are useful for clarifying the complex characteristics of large celestial phenomena, including quark stars, pulsars, neutron stars, and other extremely dense objects.

The stationary axisymmetric solutions of Einstein's equations are essential to understanding the gravitational field around astrophysical objects in general relativity. Within this category, the black hole solutions and their extensions with Maxwell fields constitute an important subset. For the past several decades, a great deal of research has focused on finding these precise solutions. The fact that the repertoire of known precise solutions has significantly expanded since Ernst's seminal discovery of a sophisticated representation of the field equations is particularly noteworthy. This novel method made it easier to investigate the symmetries included in these solutions, which stimulated more research. In the end, these investigations cleared the path for the creation of methods for producing new solutions, enabling researchers to find fresh answers by utilizing preexisting seed.

Albert Einstein presented the fundamental principles of the Einstein field equations more than a century ago, in 1915. Since then, the application of these equations has made them essential fundamentals of theoretical physics. The Einstein field equation in vacuum has the form [68]:

$$R_{\mu\nu} - \frac{1}{2}Rg_{\mu\nu} = 0 \tag{4.1}$$

For non-vacuum space-time, it can be shown that EFEs take the forms of[68]:

$$R_{\mu\nu} - \frac{1}{2}Rg_{\mu\nu} + \lambda g_{\mu\nu} = -kT_{\mu\nu} \tag{4.2}$$

where $\lambda$ is cosmological constant, $R_{\mu\nu}$is Ricci tensor, R Curvature scalar, G Newton's constant, $T_{\mu\nu}$ energy-momentum tensor, $g_{\mu\nu}$ general metric tensor and $k = \frac{8\pi G}{c^4}$ . The Einstein field equation for non zero cosmological constant can be written as

$$G_{\mu\nu} + \lambda g_{\mu\nu} = \frac{8\pi G}{c^4} \tag{4.3}$$

where the Einstein tensor $G_{\mu\nu} = R_{\mu\nu} - \frac{1}{2}Rg_{\mu\nu}$ ; The inclusion of a non-zero cosmological constant, denoted by $\lambda$, serves a crucial role in preventing a universal gravitational collapse. These equations intricately detail the interplay between the geometry of spacetime and the distribution of matter and radiation, serving as the fundamental framework of Einstein's general theory of gravity.

### 4.1.1 Schwarzschild Metric

In Einstein's theory of general relativity, the Schwarzschild metric (also known as the Schwarzschild solution) is an exact solution to the Einstein field equations that describes the gravitational field outside a spherical mass, on the assumption that the electric charge of the mass, angular momentum of the mass, and universal cosmological constant are all zero [69]. The solution is a useful approximation for describing slowly rotating astronomical objects such as many stars and planets, including Earth and the Sun. It was found by Karl Schwarzschild in 1916. According to Birkhoff's theorem, the Schwarzschild metric is the most general spherically symmetric vacuum solution of the Einstein field equations. A Schwarzschild black hole or static black hole is a black hole that has neither electric charge nor angular momentum (non-rotating). A Schwarzschild black hole is described by the Schwarzschild metric, and cannot be distinguished from any other Schwarzschild black hole except by its mass [69].

The Schwarzschild black hole is characterized by a surrounding spherical boundary, called the event horizon, which is situated at the Schwarzschild radius ($r_s$), often called the radius of a black hole. The boundary is not a physical surface, and a person who fell through the event horizon (before being torn apart by tidal forces) would not notice any physical surface at that position; it is a mathematical surface which is significant in determining the black hole's properties. Any non-rotating and non-charged mass that is smaller than its Schwarzschild radius forms a black hole. The solution of the Einstein field equations is valid for any mass M, so in principle (within the theory of general relativity) a Schwarzschild black hole of any mass could exist if conditions became sufficiently favorable to allow for its formation [70].

In a coordinate system characterized by coordinates (r, $\theta$, $\phi$, t) denoted as 1 to 4 respectively, This analysis is initiated with the metric expressed in its comprehensive form consisting of 10 independent components, each representing a continuous function of four variables. The scenario under consideration assumes spherical symmetry, staticity, and a vacuum environment.

The first simplification to be made is to diagonalize the metric. under the coordinate transformation (r, $\theta$, $\phi$, t) $\rightarrow$ ( r, $\theta$, $\phi$, -t) all metric components should remain the same.

Hence the metric must be of the form

$$ds^2 = g_{11}dr^2 + g_{22}d\theta^2 + g_{33}d\phi^2 + g_{44}dt^2 \tag{4.4}$$

Under the static assumption, the four metric components are time-independent with respect to the coordinate t. By virtue of spherical symmetry, the metric coefficients $g_{11}$ and $g_{44}$ are solely functions of the radial coordinate r. Consequently, $g_{11} = A(r)$ and $g_{44} = B(r)$

The line element for a 2- sphere in spherical coordinates is given by :

$$dl^2 = r_o^2(d\theta^2 + \sin^2\theta d\phi^2)$$

The presence of spherical symmetry on hypersurfaces at constant $r = r_o$ leads to the disappearance of off-diagonal terms in the metric.

simplifying it to

$$ds^2 = g_{22}d\theta^2 + g_{33}d\phi^2 \tag{4.5}$$

Hence $g_{22} = r^2$ and $g_{33} = r^2 \sin^2\theta$, this restructuring allows the metric to be expressed as

$$ds^2 = A(r)dr^2 + r^2 d\theta^2 + r^2 sin^2\theta d\phi^2 + B(r)dt^2 \quad (4.6)$$

Using the field equations and the weak field approximation, the schwarzschild metric can be written in the form [69]

$$ds^2 = \left(1 - \frac{2GM}{c^2 r}\right)^{-1} dr^2 + r^2\left(d\theta^2 + \sin^2 d\phi^2\right) - c^2\left(1 - \frac{2GM}{c^2 r}\right) dt^2 \quad (4.7)$$

where, $\frac{2GM}{c^2} = r_s$

$$ds^2 = \left(1 - \frac{r_s}{r}\right)^{-1} dr^2 + r^2\left(d\theta^2 + \sin^2 d\phi^2\right) - c^2\left(1 - \frac{r_s}{r}\right) dt^2 \quad (4.8)$$

In the following years, generalizing Shwarzschild's solution to include electrical charge resulted in the Reissner-Nordstrom equation [71]:

$$ds^2 = \left(1 - \frac{r_s}{r} + \frac{r^2Q}{r^2}\right) c^2 dt^2 - \left(1 - \frac{r_s}{r} + \frac{r^2Q}{r^2}\right)^{-1} dr^2 - r^2 d\Omega^2 \quad (4.9)$$

Where

$$r^2Q = \frac{Q^2G}{4\pi\epsilon c^4}$$

$$d\Omega^2 = d\theta^2 + \sin^2\theta d\phi^2$$

Schwarzschild discovered two precise solutions to Einstein's field equation: the exterior solution, which pertains to the region outside a celestial body, and the interior solution, which provides an approximation of the conditions within the body. The exterior Schwarzschild solution is not a simplistic or idealized scenario, but rather a physically significant model that accurately describes the gravitational field around spherically symmetric objects such as planets and stars. This solution is crucial for understanding various relativistic effects within the planetary system [69].

### 4.1.2 Kerr Metric

The Kerr metric is a generalization to a rotating body of the Schwarzschild metric, discovered by Karl Schwarzschild in 1915, which described the geometry of spacetime around an uncharged, spherically symmetric, and non-rotating body. However, the exact solution for an uncharged, rotating black hole, the Kerr metric, remained unsolved until 1963, when it was discovered by Roy Kerr [72, 73]. The natural extension to a charged, rotating black hole, the Kerr-Newman metric, was discovered shortly thereafter in 1965. according to the Kerr metric, a rotating body should exhibit frame-dragging (also known as Lense-Thirring precession), a distinctive prediction of general relativity. The first measurement of this frame dragging effect was done in 2011 by the Gravity Probe B experiment. Roughly speaking, this effect predicts that objects coming close to a rotating mass will be entrained to participate in its rotation, not because of any applied force or torque that can be felt, but rather because of the swirling curvature of spacetime itself associated with rotating bodies. In the case of a rotating black hole, at close enough distances, all objects even light must rotate with the black hole; the region where this holds is called the ergosphere. The light from distant sources can travel around the event horizon several times (if close enough); creating multiple images of the same object. To a distant viewer, the apparent perpendicular distance between images decreases at a factor of $e^{2\pi}$ (about 500). However, fast spinning black holes have less distance between multiplicity images [74].

Rotating black holes have surfaces where the metric seems to have apparent singularities; the size and shape of these surfaces depends on the black hole's mass and angular momentum. The outer surface encloses the ergosphere and has a shape similar to a flattened sphere. The inner surface marks the event horizon; objects passing into the interior of this horizon can never again communicate with the world outside that horizon. However, neither surface is a true singularity, since their apparent singularity can be eliminated in a different coordinate system. The Kerr metric is commonly expressed in one of two forms, the Boyer-Lindquist form and the Kerr-Schild form. It can be readily derived from the Schwarzschild metric, using the Newman-Janis algorithm [75] by Newman-Penrose formalism (also known as the spin–coefficient formalism), [76] Ernst equation, [77] or Ellipsoid coordinate transformation [78].

The Kerr black hole is axially symmetric but not spherically symmetric (that is rotationally symmetric about one axis only, which is the angular-momentum axis), and is characterized by two parameters, M and J. Since J has dimension $m^2$, conventionally defined as [68]

$$a = \frac{J}{M} \tag{4.10}$$

Which then has the dimensions as M. The line element is

$$ds^2 = g_{tt}dt^2 + 2g_{t\phi}dtd\phi + g_{rr}dr^2 + g_{\theta\theta}d\theta^2 + g_{\phi\phi}d\phi^2 \tag{4.11}$$

$$\begin{aligned} ds^2 = &-\frac{\triangle - a^2\sin^2\theta}{\rho^2}dt^2 - 2a\left[\frac{2Mr\sin^2\theta}{\rho^2}\right]dtd\phi \\ &+ \frac{(r^2+a^2)^2 - a^2\triangle\sin^2\theta}{\rho^2}\sin^2\theta d\phi^2 + \frac{\rho^2}{\triangle}dr^2 + \rho^2 d\theta^2 \end{aligned} \tag{4.12}$$

The metric components are

$$g_{tt} = -\frac{\Delta - a^2\sin^2\theta}{\rho^2} \tag{4.13}$$

$$g_{t\phi} = -\frac{2aMr\sin^2\theta}{\rho^2} \tag{4.14}$$

$$g_{rr} = \frac{\rho^2}{\Delta} \tag{4.15}$$

$$g_{\theta\theta} = \rho^2 \tag{4.16}$$

$$g_{\phi\phi} = \frac{\sin^2\theta}{\rho^2}\left[(r^2+a^2)^2 - a^2\triangle\sin^2\theta\right] \tag{4.17}$$

Where

$$\triangle = r^2 - 2Mr + a^2$$

$$\rho^2 = r^2 + a^2\cos^2\theta$$

The coordinates are called Boyer-Lindquist coordinates. Cartesian-like coordinates can be transformed in to Boyer- Lindquist coordinates as

$$x = \sqrt{r^2+a^2}\sin\theta\cos\phi$$

$$y = \sqrt{r^2+a^2}\sin\theta\sin\phi$$

$$z = r\cos\theta$$

The Kerr metric describes the geometry of spacetime in the vicinity of a mass (M) rotating with angular momentum ( J) [79].
The Kerr-Newman metric describes the geometry of spacetime in vicinity of rotating mass M with charge Q. The formula for this metric depend upon what coordinates or coordinate conditions are selected. and it can be solved starting from equation (4.9).
The kerr-Newmann metric is a generalization of the Reissner- Nordstrom metric and is given by

$$\begin{aligned} ds^2 = &-\left[\frac{\Delta - a^2\sin^2\theta}{\rho^2}\right]dt^2 - \frac{2a\sin^2\theta\,(r^2+a^2-\Delta)}{\rho^2}dtd\phi \\ &+\left[\frac{(r^2+a^2)^2-\Delta a^2\sin^2\theta}{\rho^2}\right]\sin^2\theta d\phi^2 + \frac{\rho^2}{\Delta}dr^2 + \rho^2 d\theta^2 \end{aligned} \tag{4.18}$$

The metric components are

$$g_{tt} = -\left[\frac{\Delta - a^2\sin^2\theta}{\rho^2}\right] \tag{4.19}$$

$$g_{t\phi} = -\frac{2a\sin^2\theta\,(r^2+a^2-\Delta)}{\rho^2} \tag{4.20}$$

$$g_{\phi\phi} = \left[\frac{(r^2+a^2)^2-\Delta a^2\sin^2\theta}{\rho^2}\right]\sin^2\theta \tag{4.21}$$

$$g_{rr} = \frac{\rho^2}{\Delta} \tag{4.22}$$

$$g_{\theta\theta} = \rho^2 \tag{4.23}$$

And the non zero Christoffel symbols are given by

$$\Gamma^t_{tt} = \frac{r\Delta - (r^2+a^2)(Mr-Q^2)}{2\rho^4} \tag{4.24}$$

$$\Gamma^t_{\phi\phi} = \frac{2aMr\sin^2\theta}{\rho^4} \tag{4.25}$$

$$\Gamma^t_{t\phi} = \frac{(2Mr-Q^2)a\sin^2\theta}{\rho^4} \tag{4.26}$$

$$\Gamma^r_{rr} = \frac{\Delta}{\rho^2} \tag{4.27}$$

$$\Gamma^\theta_{\theta r} = -r \tag{4.28}$$

$$\Gamma^\theta_{\theta\theta} = \frac{-\sin\theta\cos\theta}{\rho^2} \tag{4.29}$$

$$\Gamma^{\phi}_{t\phi} = \frac{Mr - Q^2}{\rho^4} \tag{4.30}$$

$$\Gamma^{\phi}_{\phi t} = \frac{(2Mr - Q^2)a\sin^2\theta}{\rho^4} \tag{4.31}$$

$$\Gamma^{\phi}_{\phi\phi} = -\frac{\Delta - a^2\sin^2\theta}{\rho^2} \tag{4.32}$$

Where

$\rho^2 = r^2 + a^2\cos^2\theta$

$\Delta = r^2 - 2Mr + a^2 + Q^2$

## 4.2 Radiative Transfer Equation

The most general form of the RTE in curved spacetime involves the Boltzmann transport equation, it can be formulated as [80]

$$\frac{\partial f^{\nu}}{\partial \tau} = j^{\nu} - k_{\alpha} f^{\nu} + \epsilon^{\nu} \tag{4.33}$$

Where

$f^{\nu}(x^{\mu})$ is specific intensity of radiation at frequency $\nu$ and spacetime point $x^{\mu}$

$\tau$ is the proper time along the ray path

$J^{\nu}$ is source term representing emission and scattering of radiation

$k_{\alpha}$ is the total opacity due to absorption and scattering of radiation

$\epsilon_{\nu}$ is the emission term representing additional radiation sources.

Emission and absorption processes act as sources and sinks for radiation within the medium traversed by the light ray. In the absence of these processes ($J^{\nu} = \epsilon^{\nu} = 0$), the specific intensity along the ray path remains constant. For certain scenarios, the full equation can be simplified Following von 2006: [81], when neglecting the effects of spacetime curvature and assuming a straight-line ray path, the equation can be written as:

$$\frac{dI_{\nu}}{ds} = -\alpha_{\nu} I_{\nu} + j_{\nu} \tag{4.34}$$

where $I_{\nu}$ is the specific intensity of the ray at a frequency $\nu$. $\alpha_{\nu}$ and $j_{\nu}$, the absorption and emission coefficients at a frequency $\nu$.

The optical depth (optical thickness of the medium between s and $s_o$ ) is given by,

$$\tau(s) = \int_{s_o}^{s} \alpha_\nu(s) ds' \tag{4.35}$$

By using the above equation the radiative equation can be written as

$$\frac{dI_\nu}{d\tau_\nu} = -I_\nu + s_v \tag{4.36}$$

where $s_v = \dfrac{j_v}{a_v}$ is the source function. Direct integration of the equation yields

$$I_v(s) = I_v(s_0) \exp^{-\tau\nu} + \int_{so}^{s} j_v(s') \exp^{-(\tau_\nu(s) - \tau_\nu(s'))} ds'$$

$$I_v(s) = I_v(s_0) \exp^{-\tau\nu} + \int_{so}^{s} s_v(\tau'_\nu) \exp^{-(\tau_\nu - \tau'_\nu)} d\tau'_\nu \tag{4.37}$$

Where the constant $I_v(s_0)(= I_v(0))$ is the initial value of the specific intensity

The general covariant radiative transfer equation can be derived from the basic principles based on the conservation of particles in phase space. The particle number density in the phase volume element [81]

$$f(x^i, p^i) = \frac{dN}{dV} \tag{4.38}$$

is an invariant quantity along the affine parameter $\lambda$; where $dN$ is the number of particles and $dV$ is volume phase space which is given by:

$$dV = d^3x d^3p$$

Liouville's theorem ensures that the phase space volume, which is unchanged along the affine parameter $\lambda$ i.e.

$$\frac{dV}{d\lambda} = 0$$

For relativistic particles, $|p| = E$, and $d^3p = E^2 dE d\Omega$ and the volume element of a bundle of relativistic particles is given by $d^3x = dAdt$. From this, the phase space density of a bundle of relativistic particles of (4.38) is written as

$$f(x^i, p^i) = \frac{dN}{E^2 dAdtdEd\Omega} \tag{4.39}$$

) where $dA$ is the area element of the bundle, $\Omega$ is the spherical solid angle [42, 82]. The specific intensity of the photon is given by:

$$I_\nu = \frac{EdN}{dAdtdEd\Omega} \tag{4.40}$$

By inspection of (4.39) and (4.40)

$$F = \frac{I_\nu}{E^3} = \frac{I_\nu}{\nu^3}$$

The lorentz invariant intensity, $I = F$ will be used to formulate the general radiative transfer formulation.

In a linear medium, the amount of energy absorbed is proportional to the radiation intensity, and the emission is independent of the intensity of the incoming radiation. Neglecting scattering, the stationary radiative transfer equation is therefore

$$\frac{dI}{ds} = -XI + \eta(\frac{\nu_0}{\nu})^3 \tag{4.41}$$

where $X$ is the absorption coefficient, $\eta$ is the emission coefficient and $ds$ is the length element that the ray traverses. The equation in this form is defined in the observer's frame.

The absorption and emission coefficients are related to their counterparts in the rest frame with respect to the medium via

$$X = (\frac{\nu_0}{\nu})X_0 \tag{4.42}$$

$$\eta = (\frac{\nu_0}{\nu})^2\eta_0 \tag{4.43}$$

where the subscript "0" denotes quantities in the local rest frame.

The relative energy (frequency) shift in a moving medium with respect to an observer at infinity is given by

$$\frac{E_0}{E} = \frac{\nu_0}{\nu} = \frac{\kappa_\beta u^\beta|_\lambda}{\kappa_\alpha u^\alpha|_\infty} \tag{4.44}$$

where $u^\alpha$ is the four-velocity of the medium as measured by an observer $\kappa_\alpha$ is the four-momentum of the photon. Define

$$\frac{ds}{d\lambda} = -||(g^{\alpha\beta} + u^\alpha u^\beta)\kappa_\alpha|| \ |_\infty \tag{4.45}$$

$$= -\sqrt{\kappa_\alpha\kappa^\alpha + 2\kappa_\alpha\kappa_\beta u^\alpha u^\beta + u^\alpha\kappa_\alpha u^\beta u_\beta + u^\alpha\kappa_\alpha} \ |_\alpha \tag{4.46}$$

$$= -\kappa_\alpha u^\alpha|_\infty \tag{4.47}$$

Because all the terms except for (4.47) vanish at infinity

It follows that the radiative transfer equation in the co-moving frame:

$$\frac{dI}{d\lambda} = -\kappa_\alpha u^\alpha|_\lambda \left[-X_0(X^\beta,\nu)I + \eta_0(X^\beta,\nu)\right] \tag{4.48}$$

$$\frac{dI}{d\lambda} = \kappa^\alpha \frac{\partial I}{\partial x^\alpha} - \Gamma^\alpha_{\beta\gamma}\kappa^\gamma \frac{\partial I}{\partial \kappa^\alpha} \tag{4.49}$$

The metric and the initial conditions define the rays (the photon trajectories in 3D space), and the solution can be obtained by direct integration along the ray. For simplicity, by assuming that the refractive index ($n = 1$) throughout the medium, the solution to equation (4.48) is then

$$I(\lambda) = I(\lambda_0)exp\left(\int_{\lambda'}^{\lambda} x_0(\lambda',\nu_0)\kappa_\alpha u^\alpha|_{\lambda"}\, d\lambda"\right)\eta_0(\lambda',\nu_0)\kappa_\alpha u^\alpha|_{\lambda'}\, d\lambda' \tag{4.50}$$

If there is a varying refractive index in the medium, then the light will be described by a dispersion relation which modifies its propagation. The equations of motion become [83]

$$\dot{x}^\alpha = \frac{\partial \nu}{\partial \kappa_\alpha} \tag{4.51}$$

$$\dot{\kappa}^\alpha = \frac{\partial \nu}{\partial x_\alpha} \tag{4.52}$$

### 4.2.1 Pressure supported accretion tori

Accretion tori resemble stars that have an atmosphere with an optical depth gradient. While emission from an opaque torus stems from an unobscured skin (surface) layer of the torus, emission from a translucent or an optically thin accretion torus is formed by the emission contribution from all regions within the torus. The thermodynamic and hydrodynamic structures of the torus determine the spectral properties of its emission, and so they must be determined prior to performing the radiative transfer calculations. To model the internal structure of the accretion tori, the tori considered as stationary and axisymmetric [84]. They consist of a perfect fluid, and the stress energy-momentum tensor of the flow is given by [81]

$$T^{\alpha\beta} = (\rho + p + \epsilon)\, u^\alpha u^\beta + p g^{\alpha\beta} \tag{4.53}$$

Where $p$ is the pressure, $\rho$ is the density and $\epsilon$ is the fluid internal energy. Because $T^{\alpha\beta}{}_{;\beta}$ = 0, it leads to

$$(\rho + p + \epsilon)_{,\beta} u^\alpha u^\beta + (\rho + p + \epsilon)\left(u^\alpha{}_{;\beta} u^\alpha + u^\alpha u^\beta{}_{;\alpha}\right) + p_{,\beta} g^{\alpha\beta} = 0 \tag{4.54}$$

Projection perpendicular to the velocity with projection tensor $p^{\alpha\beta}$ that is given by

$$p^{\alpha\beta} = g^{\alpha\beta} - u^\alpha u^\beta$$

Yields the momentum equation

$$(\rho + p + \epsilon) u^\alpha{}_{;\beta} u^\beta + p_{,\beta} g^{\alpha\beta} = 0 \tag{4.55}$$

The resulting equation (4.55) expresses the balance between the spatial part of the momentum and the forces acting on the fluid element.
Because the torus is stationary and axisymmetric, it has neglegible poloidal flow components

Hence

$$u_\beta{}_{;\alpha} u^\alpha = -\Gamma^\delta_{\alpha\beta} u_\alpha u^\beta = -\frac{1}{2} u^\alpha u^\beta g_{\delta\beta,\alpha} \tag{4.56}$$

Since $u^\alpha u_\alpha = -1$ and differentiating with respect to $\delta$

$$(u^\alpha u^\alpha)_{,\delta} = g_{\alpha\beta,\delta} u^\alpha u_\alpha + 2u^\alpha u_{\alpha,\delta} = 0 \tag{4.57}$$

This gives

$$u^\alpha u_{\alpha,\delta} = -\frac{1}{2} u^\alpha u_\alpha g_{\alpha\beta,\delta} \tag{4.58}$$

Then it follows that

$$u^\alpha{}_{;\beta} u_\beta = u^\beta u_{\beta,\alpha} = u^t \partial_\alpha u_t + u^\phi \partial_\alpha u_\phi \tag{4.59}$$

Where $\partial_\alpha$ is the gradient in the $x^\beta$ direction. For purely circular motion $(u^\alpha = u^t(1, 0, 0, \Omega))$, the coordinate angular velocity on the fluid $\Omega$ and specific angular momentum $(l)$ are defined as [85]

$$\Omega = \frac{u^\phi}{u^t} = \frac{d\phi}{dt}, \qquad l = -\frac{u^\phi}{u^t} \tag{4.60}$$

Therefore,

$$\frac{\Omega}{1-l\Omega} = u^{\phi}u_t = \Omega\left(u^t u_t\right) \tag{4.61}$$

The gradient of $l$ is

$$\partial_\alpha l = \frac{u_\phi}{{u_t}^2}\partial_\alpha u_t - \frac{1}{u^t}\partial_\alpha u^\phi \tag{4.62}$$

It follows that

$$\frac{\Omega}{1-l\Omega}\partial_\alpha l = \frac{1}{u_t}\partial_\alpha u_t + u^t\partial_\alpha u_t + u^\phi\partial_\alpha u^\phi \tag{4.63}$$

Equation (4.59) can now be expressed as

$$u_\alpha;_\beta\, u^\beta = \frac{\Omega}{1-l\Omega}\partial_\alpha l - \frac{1}{u_t} \tag{4.64}$$

Thus,

$$\frac{\partial_\alpha p}{\rho+p+\epsilon} = \partial_\alpha \ln(u_t) - \frac{\Omega}{1-l\Omega}\partial_\alpha l \tag{4.65}$$

To fully describe the system, the relationship between pressure and density of the gas (called an equation of state) is needed. The gas Will be assumed to behaves in a specific way where pressure depends only on density (a barotropic fluid). Because the equations describing the black hole (Kerr metric) are complex, typically it is solved by using numerical methods on computers. However, there's a simpler solution with a constant value for a specific quantity (denoted by $l$). This special case corresponds to a torus on the brink of instability (marginally stable) [81]

$$\int_0^p \frac{dp'}{\rho+p'+\epsilon} = \ln(u_t) - \ln(u_t)_{inner} \tag{4.66}$$

where $\ln(u_t)_{inner}$ is evaluated at the inner edge of the torus.

The analysis requires both the emissivity and opacity of the torus to be explicitly defined throughout its volume. Emissivity refers to how much radiation the material emits at each point, while opacity describes how effectively it blocks incoming radiation. Since the transparency of the torus to radiation is a key factor, these properties must be determined before simulating the radiative transfer process. In simpler terms, researchers need to know how much radiation the gas emits and absorbs at each location within the torus, along with the gas's motion and temperature distribution. This information is crucial for accurately calculating how radiation travels through the torus [81].

The total pressure within the torus is the sum of the gas pressure and the radiation pressure

$$p = p_{gas} + p_{rad} \tag{4.67}$$

Where

$$p_{gas} = \frac{\rho\kappa T}{\mu m_H} = \beta p$$

,

$$p_{rad} = \frac{4\sigma}{3c}T^4 = (1-\beta)\,p \tag{4.68}$$

When $\kappa$ is the boltzmann constant, $\mu$ is the mean molecular weight, $m_H$ the mass of hydrogen , $\beta$ the radiation of gas pressure to total pressure and $\sigma = \dfrac{\pi^2\kappa^4}{60\hbar^3c^2}$ is the black-body emittance constant.

Elliminating $\kappa T$ in the above equation yields

$$p = \hbar c\left[\frac{45(1-\beta)}{\pi^2(\mu m_H\beta)^4}\right]^{1/3}\rho^{4/3} \tag{4.69}$$

For a polytropic equation of state pressure (p) is given by

$$p = \kappa\rho^{\Gamma} \tag{4.70}$$

The internal is related to the pressure by

$$\epsilon = \frac{p}{\Gamma-1} \tag{4.71}$$

Then, Equation (4.69) implies,

$$\Gamma = 4/3$$

and

$$\kappa = \hbar c\left[\frac{45(1-\beta)}{\pi^2(\mu m_H\beta)^4}\right]^{1/3}$$

Combining the momentum equation (4.55) for a perfect fluid with the (4.70) gives

$$\left(\rho + \frac{\Gamma}{\Gamma-1}p\right)a^{\alpha} = p_{,\beta}\,g^{\alpha\beta} \tag{4.72}$$

Differentiating equation (4.70) yields

$$\partial_\alpha p = \kappa\Gamma\rho^{\Gamma-1}(\partial_\alpha \rho) \tag{4.73}$$

The density structure of the torus is given by

$$\partial_\alpha \rho = -a_\alpha \left(\frac{\rho^{2-1}}{\kappa\Gamma} + \frac{\rho}{\Gamma-1}\right) \tag{4.74}$$

Introducing a new variable $\xi$ ( akin to logarithmic of temperature ) where $\xi = \ln\left(\Gamma - 1 + \Gamma\kappa\rho^{\Gamma-1}\right)$ Equation (4.74) simplifies to

$$\partial_\alpha \xi = -a_\alpha \tag{4.75}$$

Since the torus is assumed to be stationary and axisymmetric, only two variables, distance from the center $(r)$ and azimuthal angle $(\theta)$, need to be considered in the equation. The density distribution $(\rho(r,\theta))$ throughout the torus is then determined by evaluating a specific mathematical expression (line integral) along a path. This path starts at the center of the torus (where $r = r\kappa$ and density is $\rho_c$) and extends outwards to any desired location within the torus defined by its distance $(r)$ and angle $(\theta)$. By solving this integral, the density at any point within the torus can be calculated. The equation suggests that under conditions where radiative pressure governs the pressure within a torus, an approximation can be made: $(1-\beta) \approx 1$. This simplification is then applicable for further analysis [81]

$$p = \hbar c \left[\frac{45}{\pi^2(\mu m_H \beta)^4}\right]^{1/3} \rho^{4/3} \tag{4.76}$$

$$\kappa T = \hbar c \left[\frac{45}{\pi^2(\mu m_H \beta)^4}\right]^{1/3} \rho^{1/3} \tag{4.77}$$

Once the density distribution, denoted by $\rho(r,\theta)$ , is known throughout the torus, the pressure and temperature can be easily calculated.

# Chapter 5

# Result and Discussion

In this chapter we present the result of our work including the structure of Active Galactic Nuclei (AGNs) and motion in the system, AGN interaction and emission, radiative transfer processes in the vicinity of AGN . Using appropriate boundary conditions we generate numerical synthetic data using python to present in plots. Finally, our theoretical result be discussed in relation to observations.

## 5.1 Structure of AGN in kerr space time

Supermassive black holes power the incredibly bright center parts of galaxies known as active galactic nuclei (AGNs). Understanding the radiation emission and absorption around these massive objects requires an exploration of the warped spacetime they produce. This is when the components of the Kerr metric are useful. The Kerr metric, which depends on the mass and spin of the black hole [72], defines the geometry of spacetime around a rotating black hole using certain values known as metric components ($g_{tt}, g_{t\phi}, g_{rr}, g_{\theta\theta}$, and $g_{\phi\phi}$).

But in reality, in addition to mass and spin, black holes may also possess a non-zero electric charge ($Q$). This means that the geometry of spacetime needs to be explained in more detail. This implies that a more comprehensive description of spacetime geometry is required.

A more realistic depiction of the geometry is provided by the Kerr-Newman metric, which accounts for all three parameters: electric charge $(Q)$, spin $(a)$, and mass $(M)$. This is especially true for black holes that have a significant electrical component.

**Case 1:** Where the black hole possesses zero electric charge $(Q = 0)$ along with non-zero mass $(M)$ and spin $(a)$. In this case, the metric components we analyzed previously in Equation(4.12) would be relevant.

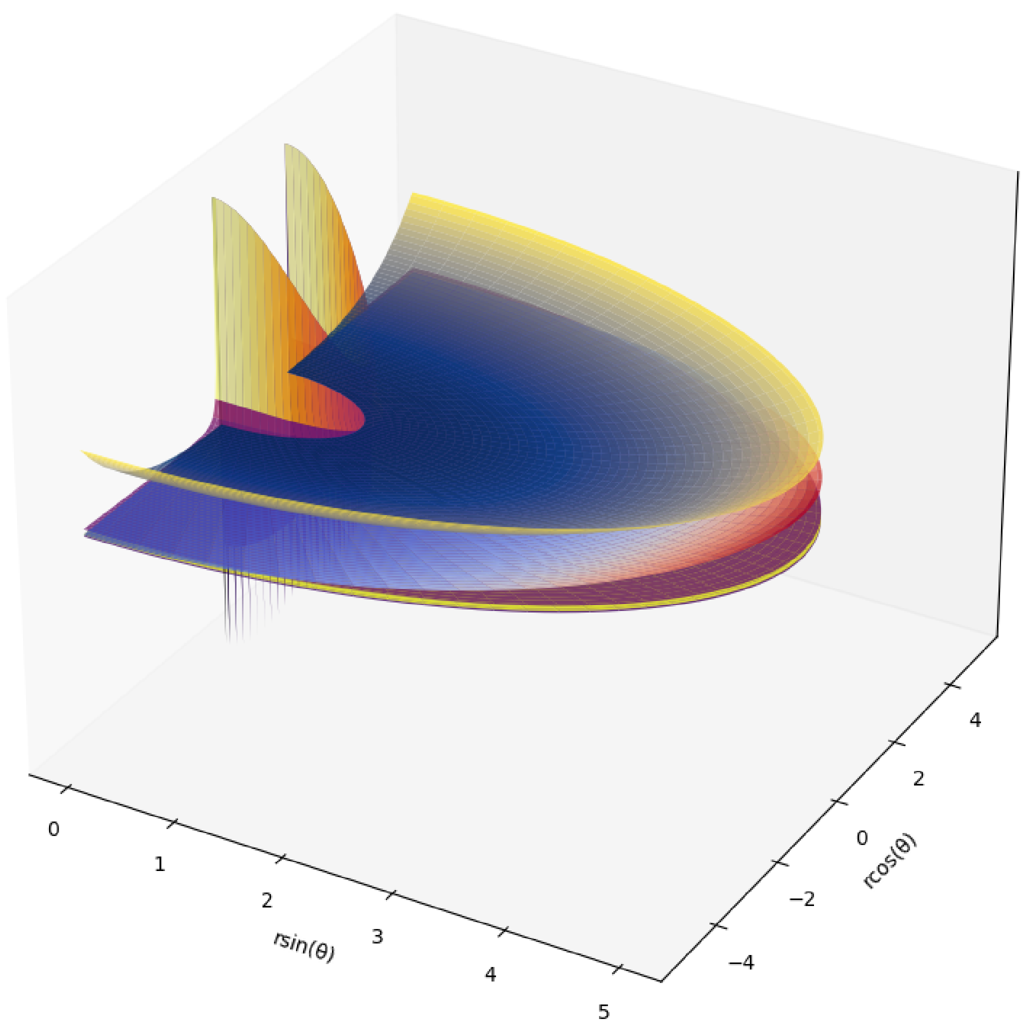


Figure 5.1: Visualization of the Kerr Metric Components for a Rotating Black Hole

**Case 2:** Where the black hole possesses a non-zero electric charge ($Q \neq 0$) along with non-zero mass ($M$) and spin ($a$).
In this case, the metric components we analyzed previously in Equation(4.17) would be relevant.

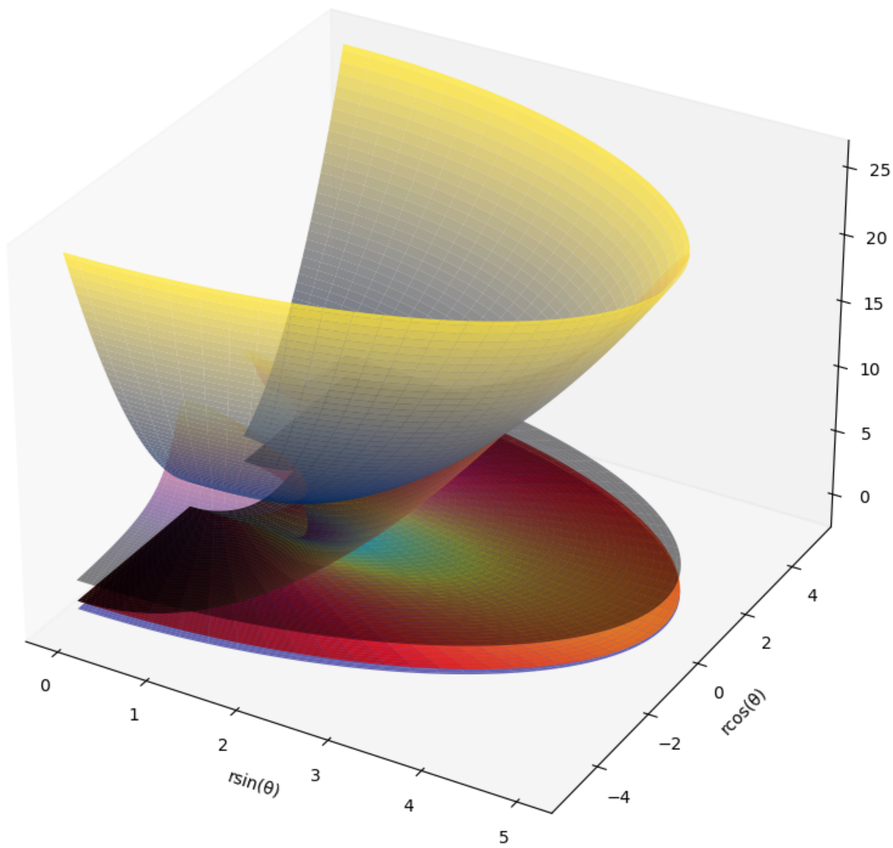


Figure 5.2: Visualization of the Kerr-Newmann Metric Components for a Rotating Black Hole

The angular momentum parameter "a" introduced by the Kerr metric creates the phenomenon of "frame-dragging," in which the spacetime itself is twisted by the black hole's rotation. The spacetime geometry around the revolving black hole is deformed in a way that resembles a cone as a result of this twisting action. The size of the black hole's angular momentum is closely correlated with the extent of this distortion.

The Kerr-Newman metric, on the other hand, extends the Kerr metric by adding the parameter ”Q” to indicate the electric charge of the black hole. This adds another level of intricacy to the deformation of spacetime. The magnetic field produced by the black hole’s rotation interacts with the electric field produced by the black hole’s electric charge. When compared to the Kerr metric alone, this combined impact causes a more complex and noticeable warping of the spacetime geometry, producing a more dramatic cone-like distortion.

The physical mechanisms controlling the emission and absorption of radiation surrounding active galactic nuclei (AGN) are greatly influenced by the Kerr-Newman metric, which characterizes the spacetime geometry around a revolving, charged black hole.
Based on Figure (5.1) and (5.2) we can develop the general discussion:

- **Time Dilation Due to Gravitation:** The $g_{tt}$ metric component significantly decreases in the vicinity of the supermassive black hole at the center of an AGN due to a strong gravitational field. This indicates that time appears to pass more slowly in the areas nearest to the black hole from a distance. Light released from the accretion disk surrounding the black hole can have significant effects on its measured properties due to this gravitational time dilation effect. In particular, as the emission and absorption processes taking place in the accretion disk slow down with respect to the distant observer’s frame of reference, photons traveling through these time-dilated regions will redshift in frequency and energy[86].
- **Rotation of Spacetime and Frame-Dragging:** The presence of frame-dragging is indicated by the $g_{t\phi}$ metric component, which becomes non-zero when the black hole in the center of an AGN is rotating. The accretion disk’s dynamics as well as the paths of matter and radiation in the black hole’s surroundings can be significantly impacted by this effect, in which the spacetime itself is ”dragged” by the spinning of the black hole. This rotation of spacetime can modify particle and photon angular momentum, which can impact the emission and absorption processes near the AGN. For instance, relativistic jets that arise as a result

of spacetime rotation have the ability to alter the perceived radiation across the electromagnetic spectrum [87].

- **Curvature of Spacetime:** The $g_{\theta\theta}$, $g_{\phi\phi}$, and $g_{rr}$. The curvature of spacetime close to the black hole is described by metric components. The trajectories that light beams and particles take can be greatly impacted by this curvature, which can result in phenomena like gravitational lensing. When photons from the accretion disk pass through areas of high curvature, they can be bent and warped. The curved spacetime modifies the photons' trajectory within the accretion disk, potentially changing their apparent properties, including polarization, energy, and frequency[88].

- **Impact on Accretion Processes:** The accreting matter's gravitational potential is strongly influenced by the distorted spacetime around the black hole, as indicated by the changing metric components. This modified potential affects the behavior and trajectory of matter as it approaches the black hole, which in turn impacts the AGN's emission properties and the efficiency of the accretion process. For example, the accretion rate and the distribution of matter in the disk can be altered by the warped spacetime, leading to changes in the observed radiation from the AGN [89].

### 5.1.1 Relativistic Equation of Motion in Kerr-Newman Spacetime

Having discussed the key astrophysical phenomena associated with charged black holes, relativistic jet formation, and radiative processes in AGN, we now turn our attention to the theoretical framework used to describe the motion of particles and photons in the vicinity of these supermassive black holes. The relativistic equation of motion in Kerr-Newman spacetime is derived using the standard variational principles, which involve extremizing the invariant geodesic element along the particle's path. The equation of motion is obtained by considering the variation of the invariant geodesic element, given by:

$$\delta \int ds = 0 \tag{5.1}$$

Here $ds$ represents the geodesic element and is given by

$$\frac{ds}{d\lambda} = \left(-g_{\mu\nu}\frac{dx^\mu}{d\lambda}\frac{dx^\nu}{d\lambda}\right)^{1/2} \tag{5.2}$$

$\lambda$ is the affine parameter along the world line.

Using polar spherical coordinates and expanding the above equation, we arrive at the following expression:

$$\delta\int\frac{1}{2}\left(g_{tt}\dot{t}^2 + 2g_{t\phi}\dot{t\phi} + g_{rr}\dot{r}^2 + g_{\phi\phi}\dot{\phi}^2\right)d\lambda = 0 \tag{5.3}$$

In this equation, the Kerr-Newman metric is employed. The Lagrangian formalism is then introduced, where the integrand in the previous equation is considered as the relativistic Lagrangian per unit mass of the system:

$$L = \frac{1}{2}\left(g_{tt}\dot{t}^2 + 2g_{t\phi}\dot{t}\phi + g_{rr}\dot{r}^2 + g_{\phi\phi}\dot{\phi}^2\right) \tag{5.4}$$

The Lagrangian plays a crucial role in the Euler-Lagrange equations of motion, which are used to derive important observable quantities related to the motion. In the Lagrangian mechanics approach, the Euler-Lagrange equations of motion are given by:

$$\frac{d}{d\lambda}\left(\frac{\partial L}{\partial\dot{x}^\mu}\right) - \frac{\partial L}{\partial x^\mu} = 0 \tag{5.5}$$

The conjugate momentum $P_\mu$ to the coordinate $x_\mu$ is given by

$$p_\mu = \frac{\partial L^\mu}{\partial\dot{x}} \tag{5.6}$$

In terms of this conjugate momentum, the Euler- lagrange equations can be recast as

$$\frac{d}{d\lambda}p_\mu = \frac{\partial L}{\partial x^\mu} \tag{5.7}$$

For the axisymmetrically static metric, $g_{\mu\nu}$ is independent of the $t$ and $\phi$ coordinates. Then,

$$\frac{\partial L}{\partial x^0} = 0 \tag{5.8}$$

$$\frac{\partial L}{\partial x^3} = 0 \tag{5.9}$$

where $x^0 = t$ and $x^3 = \phi$. Notice that, if the metric does not depend on a given coordinate $x^\mu$, the corresponding conjugate momentum is a constant of motion. Moreover, if

the metric is independent by a coordinate there is a killing vector $\xi_\mu \dot{x}^\mu$ is a constant of motion in the case of $t$ and $\phi$ for the kerr-Newmann metric.
Aiming to see the effects of rotation on the geodesics, we consider particles in an equatorial plane, where the zenith angle is $\theta = \frac{\pi}{2}$, the metric given by (4.18) is recast as

$$ds^2 = -\left[\frac{(\Delta - a^2)}{r^2}\right] dt^2 - 2a\left(r^2 + a^2 - \Delta\right) dt d\phi + \left[\frac{(r^2+a^2)^2 - \Delta a^2}{r^2}\right] d\phi^2 + \frac{r^2}{\Delta} dr^2 \quad (5.10)$$

The components of the metric given by equation (5.10) are

$$g_{tt} = -\frac{\Delta - a^2}{r^2} \quad (5.11)$$

$$g_{rr} = \frac{r^2}{\Delta} \quad (5.12)$$

$$g_{\phi\phi} = \frac{(r^2+a^2)^2 - \Delta a^2}{r^2} \quad (5.13)$$

$$g_{t\phi} = g_{\phi t} = -2a(r^2 + a^2 - \Delta) \quad (5.14)$$

Using these metrics, the Lagrangian of the system, equation (5.4), becomes

$$2L = -\left[\frac{\Delta - a^2}{r^2}\right] \dot{t}^2 - \frac{2a(r^2+a^2-\Delta)}{r^2} \dot{t}\dot{\phi} + \left[\frac{(r^2+a^2) - \Delta a^2}{r^2}\right] \dot{\phi}^2 + \frac{r^2}{\Delta}\dot{r}^2 \quad (5.15)$$

Then, the Euler- lagrange equation of motion along $t, r$ and $\phi$ are respectively given as

$$\frac{d}{d\lambda}\left(\frac{\Delta - a^2}{r^2}\right)\dot{t} + \left(2a\frac{r^2+a^2-\Delta}{r^2}\right)\dot{\phi} = 0 \quad (5.16)$$

$$\frac{d}{d\lambda}\left(\frac{r^2}{\Delta}\dot{r}\right) = \left(-2r^2 + 2Mr + 2\Delta\right)\dot{t}^2 + \frac{(4Mra - 4Q^2a)\,\dot{t}\dot{\phi} + (2r^4 - 2Mra^2 + 2Q^2a^2)}{r^3}$$
$$+ \frac{(2r\Delta - 2r^3 + 2Mr^2)}{\Delta^2}\dot{r}^2 \frac{d}{d\lambda}\frac{[(r^2+a^2)^2 - \Delta a^2]}{r^2}\dot{\phi} - \frac{a(r^2+a^2-\Delta)}{r^2}\dot{t} = 0$$
$$(5.17)$$

Since the space time of the Kerr-Newmann family is stationary and axially symmetric, the momenta $P_t$ and $P_\phi$ are conserved along the geodesics. So we obtain two constants of motion: one is corresponding to the conservation of energy ($E$) and the other is the angular momentum ($J$) about the symmetry axis, respectively given as

$$\frac{\partial L}{\partial \dot{x}^0} = -E \quad (5.18)$$

$$\frac{\partial L}{\partial \dot{x}^3} = J \quad (5.19)$$

Where

$$E = \left(\frac{\Delta - a^2}{r^2}\right)\dot{t} + \frac{a(r^2 + a^2 - \Delta)}{r^2}\dot{\phi} \tag{5.20}$$

$$J = \frac{[(r^2 + a^2)^2 - \Delta a^2]}{r^2}\dot{\phi} - \frac{a(r^2 + a^2 - \Delta)}{r^2}\dot{t} \tag{5.21}$$

Using Equations (5.20) and (5.21), the velocities along $t$ and $\phi$ are respectively given as

$$\dot{t} = \frac{-Er^2}{[(\Delta - a^2)(r^2 + a^2)^2 - \Delta a^2]} \times \frac{[(r^2 + a^2)^2 - \Delta a^2]}{[Jr^2 + a(r^2 + a^2 - \Delta)]} \tag{5.22}$$

The equation for $\dot{t}$ represents the time component of the particle's four-velocity. It depends on various parameters such as the energy of the particle $(E)$, its angular momentum $(J)$, and the properties of the black hole (mass, charge, and angular momentum). The numerator of $\dot{t}$ contains the term $-Er^2$, which represents the energy of the particle multiplied by the square of the radial coordinate $(r)$. The denominator involves terms related to the black hole's properties, including the mass, charge, and angular momentum $(a)$. Specifically, it includes factors like $(\Delta - a^2)$ and $(r^2 + a^2)^2 - \Delta a^2$ , where $\Delta$ is related to the black hole's event horizon. The equation for $\dot{t}$ provides insights into how the energy of a particle affects its radial velocity. It shows how the black hole's properties and the particle's energy determine the behavior of the particle's time component of the four-velocity

$$\dot{\phi} = \frac{[Lr^2 + a(r^2 + a^2 - \Delta)]}{[(r^2 + a^2)^2 - \Delta a^2]\,[\Delta - a^2]} \times \frac{-Er^2\,[(r^2 + a^2)^2 - \Delta a^2]}{[(r^2 + a^2)^2 - \Delta a^2]\,[2a(r^2 + a^2 - \Delta)]\,[Jr^2 + a(r^2 + a^2 - \Delta)]} \tag{5.23}$$

The numerator of $\dot{\phi}$ includes terms related to the angular momentum of the particle $(L)$ and the black hole's properties, such as mass, charge, and angular momentum $(a)$. The denominator contains factors like $(\Delta - a^2)$ and $(r^2 + a^2)^2 - \Delta a^2$, similar to the radial velocity equation.

This indicates that the azimuthal velocity of the particle is influenced not only by its own angular momentum but also by the gravitational field and rotational properties of the black hole. The interplay between these factors determines the particle's rotational motion in the vicinity of the black hole.

## 5.2 Accretion as the Main Source of Energy Release from Active Galactic Nuclei

The primary source of the intense electromagnetic radiation (EM) emitted by active galactic nuclei (AGNs) is matter accretion onto the supermassive black hole located at the center of the system. Massive gravitational potential energy is gained by matter as it spirals inward towards the black hole. This energy is subsequently dissipated, primarily by viscous dissipation, within the accretion disk to become thermal energy [90].

There would be no direct observation of any radiation released beyond the event horizon since it is a point of no return. Nonetheless, the region known as the innermost accretion disk (IAD), which is extremely near to the event horizon, is an important location for radiation generation. A large fraction of the AGN luminosity is thought to be caused by strong tidal forces and high friction within the IAD.

The equations 3.5 and 3.2 are crucial to quantify the amount of radiation processed near the event horizon. The relationship between the accretion brightness and the

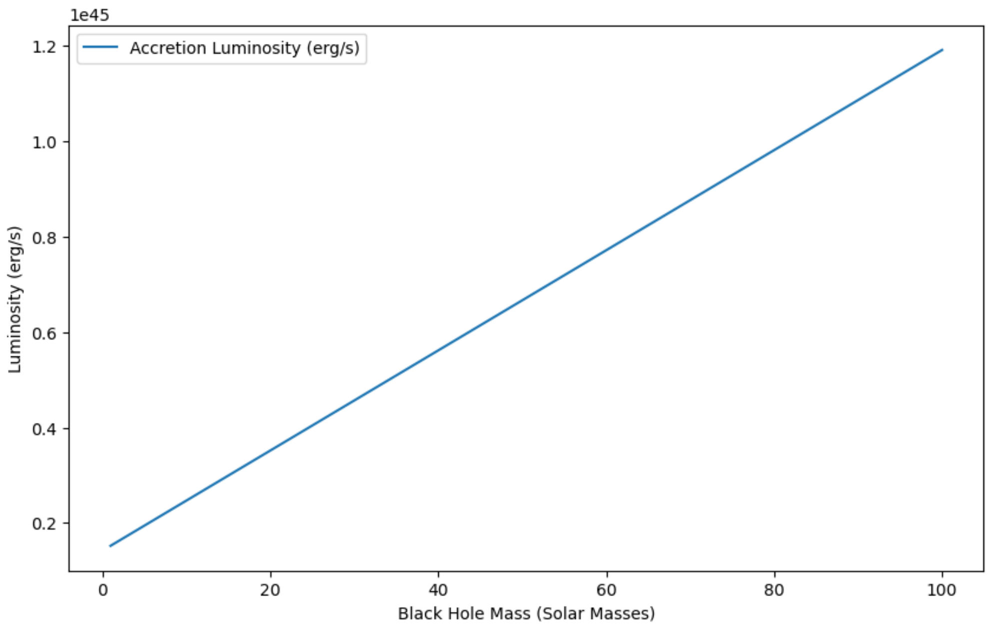


Figure 5.3: The amount of radiation processed at the event horizon

mass of the supermassive black hole is depicted in Figure 5.3. The main finding is that the accretion luminosity rises with the black hole's mass.

The following formula is used to compute the accretion luminosity:

$$L_{\text{acc}} = \eta \dot{M} c^2 \tag{5.24}$$

Where:

The accretion luminosity, or total radiation output from the accretion disk, is denoted by $L_{\text{acc}}$.

$\dot{M}$ is the mass accretion rate, or the rate at which matter is falling into the black hole;

$\eta$ is the efficiency factor, which indicates the fraction of the rest mass energy of the accreted matter that is turned into radiation.

$c$ is the speed of light

The mass-energy conversion efficiency $\eta$ is assumed to increase linearly with the black hole mass, ranging from $0.05$ for a low-mass black hole to $0.42$ for a high-mass black hole.

The range of black hole masses considered in the model spans from $10^6$ to $10^{10}$ solar masses. Supermassive black holes with masses in this range are found at the centers of most galaxies, including our own Milky Way, which is thought to host a black hole with a mass of around $4 \times 10^6$ solar masses [91].

The values of the parameters used in the calculation of the accretion luminosity are based on established astrophysical constants:

Gravitational constant ($G$) = $6.67 \times 10^{-8}$ cm$^3$ g$^{-1}$ s$^{-2}$ [92]

Speed of light ($c$) = $3 \times 10^{10}$ cm/s (exact value)

Proton mass (m$_p$) = $1.67 \times 10^{-24}$ g [92].

The linear dependence of the mass-energy conversion efficiency $\eta$ on the black hole mass is a simplified assumption, but it captures the general trend that larger black holes are expected to have higher spin and, consequently, higher radiative efficiencies [93].

The presented model and graph provide a useful framework for understanding the relationship between the black hole mass and the amount of radiation processed at the event horizon of an active galactic nucleus (AGN). This information can be valuable in the study of AGN energetics and the overall energy output of these cosmic powerhouses.

This efficient conversion of gravitational potential energy into radiation is a key factor in producing the high-energy output observed in the vicinity of the supermassive black hole. Unlike stars, where nuclear fusion is the primary energy source, nuclear fusion is insignificant in AGNs due to the extreme conditions around the black hole, making the accretion process the dominant mechanism for energy generation.

### 5.2.1 Potential Contributions of Nuclear Fusion in AGNs

Even while accretion is clearly the dominant process in AGNs, there have been talks regarding possible scenarios in which nuclear fusion could play a role: [16]

1. **Low Accretion Rates:** High temperatures and densities are necessary for nuclear fusion to occur; in AGNs with relatively low rates of accretion, the densities and temperatures inside the accretion disk may not be high enough for meaningful nuclear fusion to occur.

2. **Opacity of the Accretion Disk:** An AGN has an extremely thick, opaque accretion disk. This indicates that photons generated in the disk as a result of nuclear fusion are probably going to be rapidly absorbed and reemitted. These photons cannot escape the disk and add directly to the brightness of the AGN because of this absorption.

However, there are additional possibilities where nuclear fusion might play a tiny role in reheating the accretion disk in some AGNs:

1. **Inner Regions of the Accretion Disk:** The inner areas of the accretion disk are often hotter and denser than the outer regions. In AGNs with extremely low accretion rates, these inner regions might attain situations more suitable for nuclear fusion to occur to a limited extent.

2. **Low Accretion Rates with Less Opaque Disk:** In rare situations, AGNs with exceptionally low accretion rates might also have a less opaque accretion disk. This could allow some photons produced by nuclear fusion to escape the disk and contribute little to the AGN's overall brightness.

We can compare the energy release from the viscous dissipation by using (3.1) process within the accretion disk with the theoretical maximum energy obtainable from nuclear fusion, assuming a complete mass conversion (which is highly unlikely) according to the equation $E = Mc^2$. The inner and outer radii of the accretion disk can be approximated using the Schwarzschild radius ($R_s$) multiplied by factors of 10 and 1000, respectively [90].

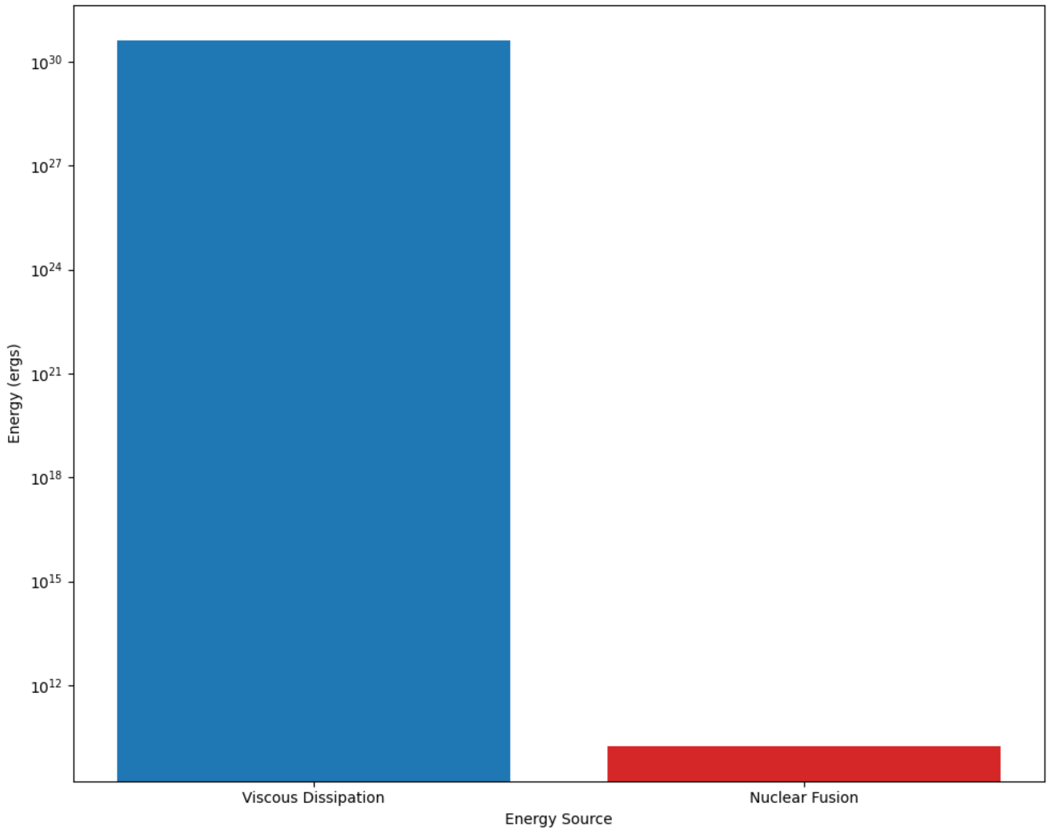


Figure 5.4: Comparison of viscous dissipation energy and nuclear fusion energy in AGN

As illustrated in Figure 5.4, the efficiency of accretion is much higher than that of nuclear fusion within the context of AGNs [90]. Our analysis's findings show that active galactic nuclei's (AGN) viscous dissipation is, in fact, very high—beyond $10^{30}$ erg/s. One of the main features of the tremendous activity taking place in the accretion disks surrounding supermassive black holes at the centers of many galaxies is this enormous quantity of energy dissipation. As much as $10^{46}$ erg/s, or 100 billion times the Sun's energy production, can be produced by the most luminous AGN [6].

The accretion of materials onto the supermassive black hole at the heart of the AGN is thought to be the source of this energy output. The graphs also show that the processed radiation, which is the energy that is finally released from the accretion disk, is very high. This radiation can interact and impact the host galaxy in a number of ways, including heating the surrounding gas, causing outflows, and changing the galaxy's evolution.

### 5.2.2 Density and Temperature profile of an AGN

Equation (3.8) gives the disk density and Equation (3.7) can be used to compute the disk temperature. The accretion disk's temperature and density profiles can be visualized with these formulae. Furthermore, by adding the Lorentz factor to the formulas, the implications of general relativity can be included.

According to the classic Shakura-Sunyaev model, temperature steadily drops as radius increases [33]. However, because of the strong gravitational effects close to the black hole, the general relativistic model shows higher temperatures in the inner disk region in the case of accretion disks around active galactic nuclei (AGN)[89]. But, To a distant observer, that light might even appear slightly "bluer" (higher frequency, seemingly hotter) compared to when it was closer to the black hole. It's not that the light itself actually gets hotter, but the bending of spacetime by gravity creates this.
The classical model exhibits a power-law-like reduction in density with radius and assumes a constant aspect ratio [33]. Compared to the classical example, the general relativistic model exhibits a faster decrease in density with radius, which is indicative of the influence of strong gravity [89].

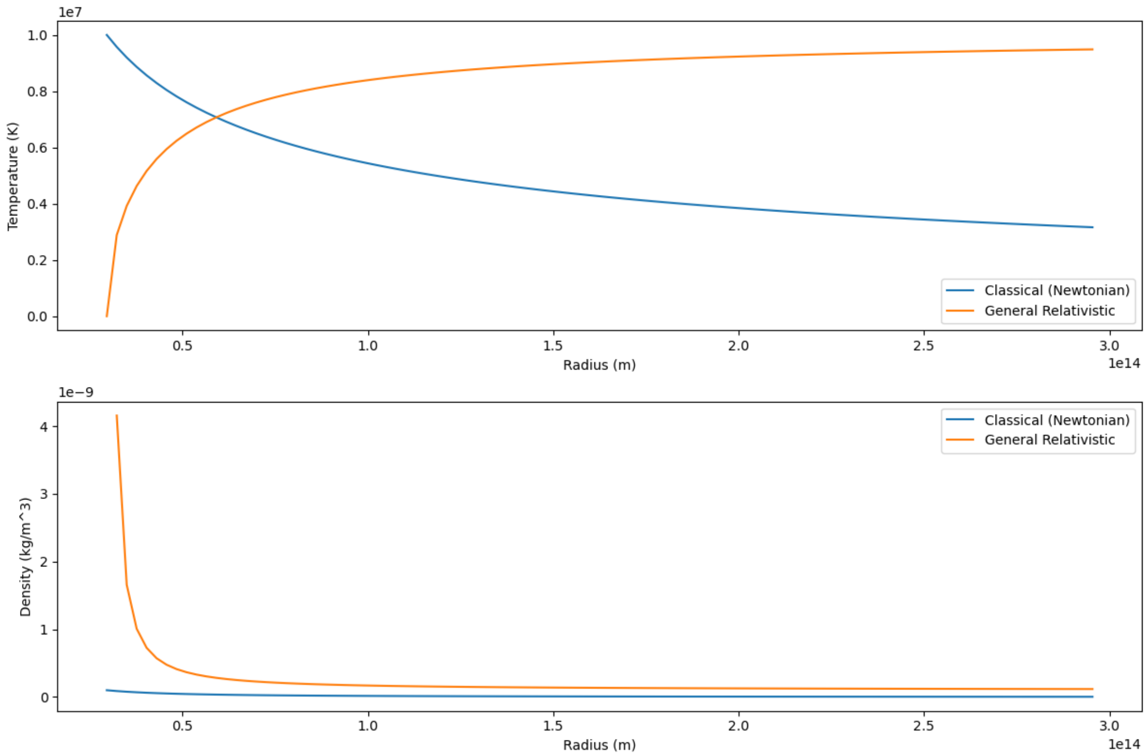


Figure 5.5: Temperature and density of an AGN

## 5.3 Radiation Transfer from AGN to Host Galaxy

Given that accretion is widely accepted as the primary energy source for Active Galactic Nuclei (AGNs), we will examine the interactions between these energetic objects' radiation and the galaxies they inhabit. We can create a more comprehensive understanding of this energy transfer process by utilizing the ideas presented in equations (3.6) and (3.11) and by examining observations made throughout the electromagnetic spectrum, from high-energy X-rays ($10^{-8}$m) to radio waves (meters and beyond) [13].

Figure 5.6 shows the theoretical spectral energy distribution (SED) of an AGN over a wide range of wavelengths, from X-rays to radio waves. The intricate blend of thermal and non-thermal emission mechanisms that define the radiation output of these active galactic nuclei is seen in this illustration.

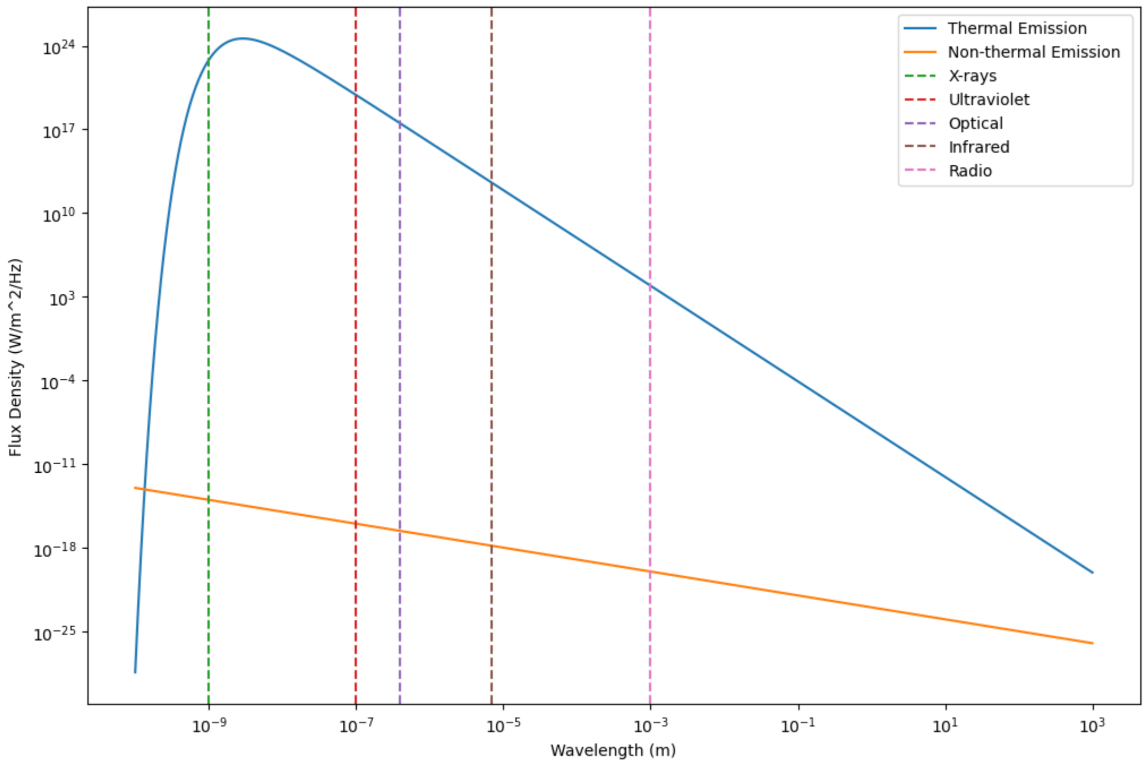


Figure 5.6: Theoretical thermal and non-thermal emission spectrum of an AGN.

### 5.3.1 Emissions, Both Thermal and Non-Thermal, in the Temperature Range of $10^5$–$10^7$ Kelvin

Thermal and non-thermal processes are the predominant emission mechanisms in the temperature range of $10^5$ to $10^7$ Kelvin. Non-thermal emission is usually connected to the acceleration of charged particles, as in the case of synchrotron radiation, whereas thermal emission is illustrated by the blackbody radiation released by the heated, ionized gas.

The Planck function (3.6) can be used to characterize the blackbody radiation for thermal emission. Thermal emission can reach levels on the order of $10^{24} erg/s/cm^2/Hz$ at the temperature of $10^7$ Kelvin [80].

The blackbody spectrum's peak moves to higher frequencies at these extraordinarily high temperatures, where it is located in the electromagnetic spectrum's ultraviolet (UV) to extreme ultraviolet (EUV) range. Significant X-ray emission can also be seen in some AGNs, even though the thermal radiation from the accretion disk is the main source of emission in these systems.

The equation (3.11) [94, 95] can be used to describe the non-thermal emission, in particular the synchrotron radiation. The non-thermal emission originates in locations with temperatures between $10^5$ and $10^7$ Kelvin, and is mostly caused by processes such as synchrotron radiation. Values of this emission can vary from roughly $10^{-15}$ to $10^{-11}$, depending on the particular type of AGN and the observed wavelength.Through a $erg/s/cm^2/Hz$ across a broad portion of the electromagnetic spectrum .

The combination of thermal and non-thermal emission processes in the temperature range of $10^5$ to $10^7$ Kelvin can provide valuable insights into the physical conditions and processes occurring in various astrophysical environments, such as the cores of massive stars, active galactic nuclei, or the early universe. The thermal emission, dominated by blackbody radiation, can be used to infer the temperature and density of the emitting regions, as well as the composition of the hot, ionized gas. The non-thermal emission, particularly the synchrotron radiation, can provide information about the presence and properties of magnetic fields, as well as the acceleration of charged particles in these extreme environments. By studying the relative contributions and spectral characteristics of the thermal and non-thermal emission, it is possible to gain a better understanding of the underlying physical processes and the overall energetics of these systems.

## 5.4 The effect of Radiative hydrodynamic transfer on the Energy output of host galaxy

### 5.4.1 Accretion Efficiency and Its Influences on the Energy output of the Host Galaxy

A higher accretion efficiency ($\eta$) has the potential to result in a more luminous active galactic nucleus (AGN), thereby intensifying the overall radiation reaching the host galaxy. This radiation has the ability to engage with the interstellar medium (ISM) of

the host galaxy through various mechanisms such as absorption, scattering, and re-emission. Consequently, these interactions significantly impact the observed spectral characteristics of the galaxy.
Furthermore, an increased bolometric luminosity ($L_{bol}$) originating from the AGN implies a larger quantity of radiated energy, which in turn augments the potential for interaction with the host galaxy.

Equation (3.2) provides a theoretical framework that enables us to quantify radiative transfer's effect on the host galaxy's energy output.

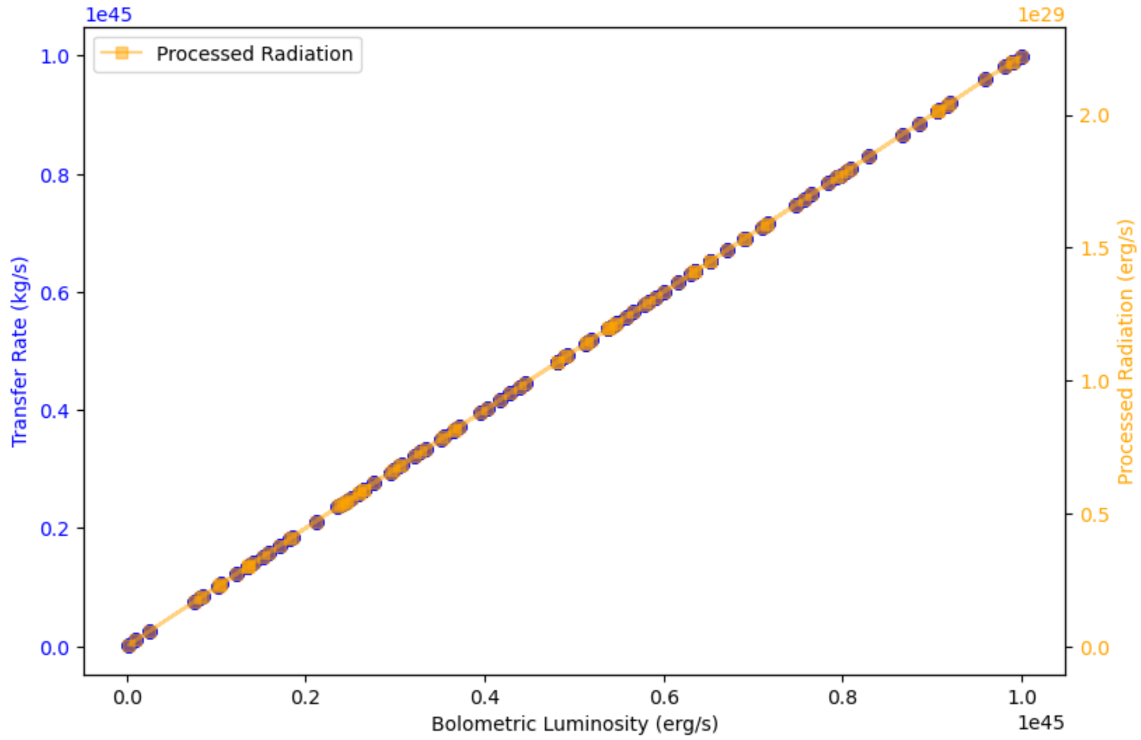


Figure 5.7: Accretion Efficiency Influence on the Energy output of the Host Galaxy

The scatter plot (Figure 5.7) illustrates the correlation between the radiative transfer rate to the host galaxy and the bolometric brightness of an Active Galactic Nucleus (AGN). The overall electromagnetic power production of the AGN over the whole spectral range is represented by the bolometric luminosity. The efficiency with which this light is transmitted and absorbed by the host galaxy around it is measured by the radiative transfer rate. This figure sheds light on the energetic interaction and exchange that occurs between the AGN driven by a central supermassive black hole and its galactic

surroundings.
An AGN with a higher bolometric luminosity is usually thought to be more energetic and able to release more radiation. The efficiency with which this radiant energy is transmitted to and impacts the host galaxy's energetic output is then characterized by the radiative transfer rate[96].

### 5.4.2 The Influence of Optical Depth on the Energy out put of the Host Galaxy

Theoretical frameworks can be used to quantify the impact of dust extinction on the radiative transmission of emission from Active Galactic Nuclei (AGNs). The foundation for simulating the effect of optical depth ($\tau$), a measure of the opacity of a material, is provided by equations (4.34) and (4.35). An extremely opaque medium is indicated by a high optical depth ($\tau \approx 1.5$, [97]), which implies a considerable dust extinction within the host galaxy. These equations can be used to create a theoretical simulation that examines the impact of dust extinction on AGN radiation transmission processes, with a representative optical depth of 1.5.

The simulation results provide significant insight on the radiative transfer effect of hydrodynamics in the host galaxy's energy output. The plot unequivocally shows that the rate of change of a given intensity is greatly influenced by varying values of optical depth ($\tau$). The rate at which a particular intensity changes decreases with increasing optical depth.

**High Depth of Focus ($\tau = 1.5$):** This case illustrates a highly opacified material in which there is a notably more likely of light absorption. With increasing distance, the plot for this scenario will show a faster drop in the rate of change of particular intensity ($\frac{di}{ds}$). This shows that the light's intensity is rapidly decreasing as it passes through the medium. Shorter wavelengths, such ultraviolet (UV) or X-rays, are especially relevant to this behavior because they are easily absorbed by the gas and dust in the medium [80].

**Low Optical Depth** ($\tau = 0.001, 0.1, 0.3, 0.5$): The scenarios depict different levels of transparency in the media. Plots for these scenarios will indicate a more progressive

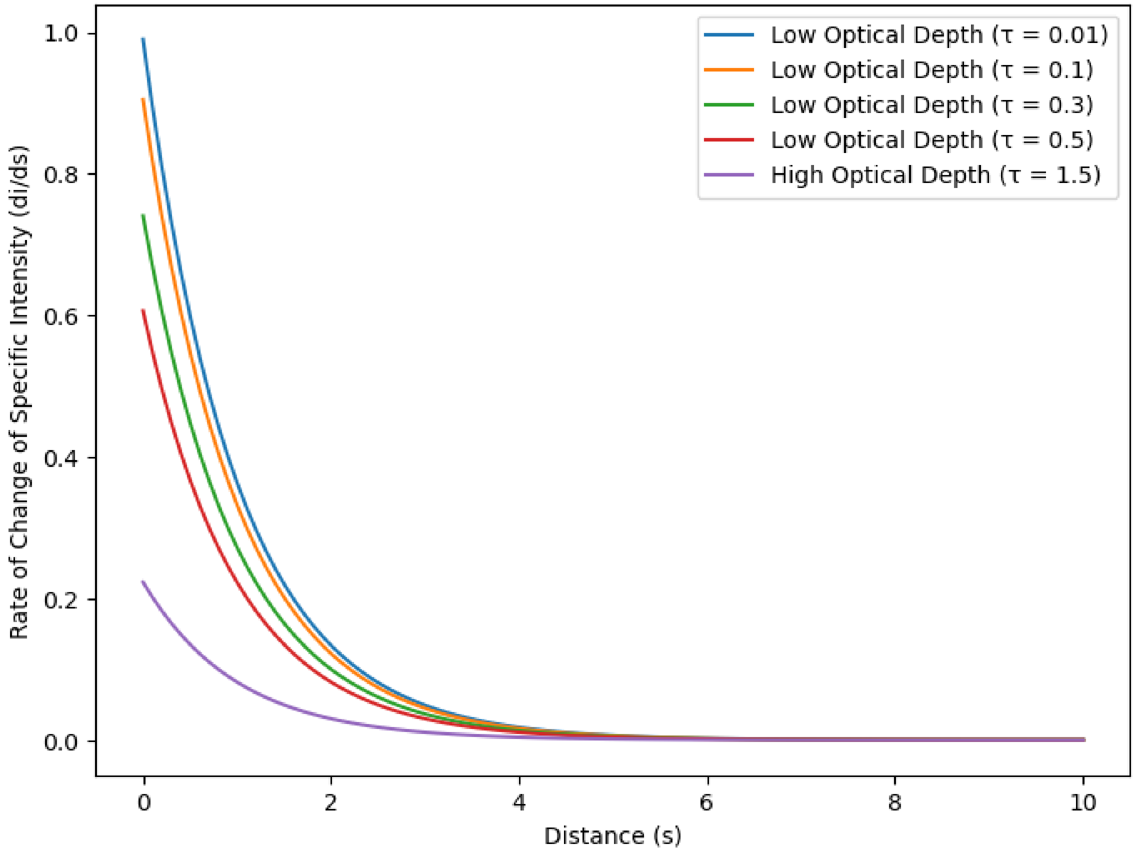


Figure 5.8: Impact of Optical Depth on Specific Intensity Change

decrease in light intensity with distance, as indicated by a more gradual decrease in $(\frac{di}{ds})$. Since longer wavelengths are less prone to absorption processes, such as visible light and near-infrared (NIR), they can pass through dust and gas clouds more readily, hence this behavior is relevant for longer wavelengths [98].

The effect of dust or the material's opacity can generally be seen in Figure 5.9 by comparing the specific intensity with the no-dust case for multi-wavelength spectra.

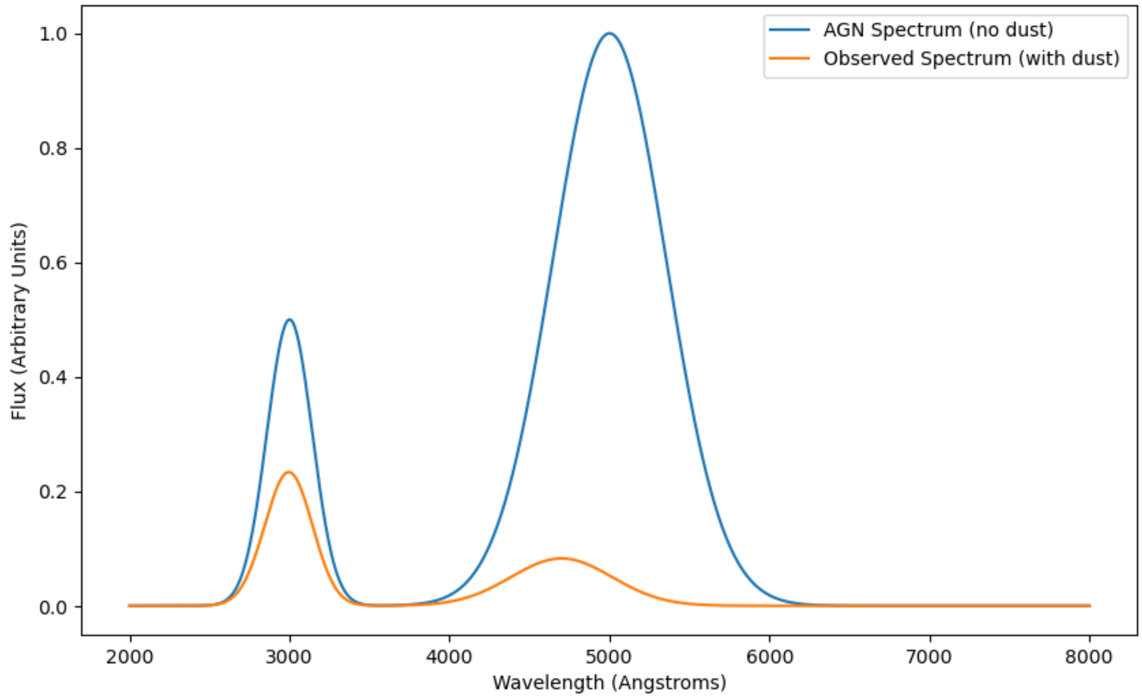


Figure 5.9: Impact of Dust on Specific Intensity Change

When the light intensity rapidly attenuates in the high optical depth condition, the radiation is more effectively absorbed by the surrounding medium, which can result in a significant reduction in the host galaxy's overall energy production. In contrast, a larger fraction of the radiation can reach the observer in the low optical depth scenarios due to the more gradual drop in light intensity, which leads to a proportionally higher energy output from the host galaxy.

# Chapter 6

# Summary and Conclusion

The physical mechanisms controlling Active Galactic Nuclei (AGNs) and their surroundings were examined in this work. Our specific objectives were to model the radiation transfer to the host galaxy, quantify the amount of radiation processed at the event horizon of the central supermassive black hole, understand the emission and absorption of radiation around AGNs, and finally simulate the combined effects of radiative transfer and hydrodynamics on the energy output of the host galaxy. We determined and examined the equations of motion for particles in the gravitational field of the AGN and described the orbits of these particles using analytical techniques. We also looked at how matter is accreted onto the black hole and how that contributes to energy conversion. In spite of this, the work lays a solid platform for future studies on AGNs and their effects on their surroundings. Given the interplay of geometry, gravity, and charge, we think it can help us understand better how energy and particles flow within and around AGNs. In the end, research on AGNs and their effects on their surroundings is still ongoing. Future investigations should focus on these interactions, especially the processes by which AGNs introduce particles and energy into their surroundings while taking geometry, gravity, and charge into account.

# Bibliography


[1] Volker Beckmann and Chris SHRADER. The agn phenomenon: open issues. page 069, 07 2013.

[2] Carl K Seyfert. Nuclear emission in spiral nebulae. In *A Source Book in Astronomy and Astrophysics, 1900–1975*, pages 738–743. Harvard University Press, 1979.

[3] John G Bolton, Gordon J Stanley, and OB Slee. Positions of three discrete sources of galactic radio-frequency radiation. In *A Source Book in Astronomy and Astrophysics, 1900–1975*, pages 777–778. Harvard University Press, 1979.

[4] Cyril Tasse. *Host galaxies and environment of active galactic nuclei: a study of the XMM large scale structure survey.* PhD thesis, Leiden University, 2008.

[5] George C Southworth. Early history of radio astronomy. *The Scientific Monthly*, 82(2):55–66, 1956.

[6] Hagai Netzer. *The physics and evolution of active galactic nuclei.* Cambridge university press, 2013.

[7] KI Kellermann. The discovery of quasars and its aftermath. *arXiv preprint arXiv:1304.3627*, 2013.

[8] Alessandro Marconi, Guido Risaliti, Roberto Gilli, Leslie K Hunt, Roberto Maiolino, and Marco Salvati. Local supermassive black holes, relics of active galactic nuclei and the x-ray background. *Monthly Notices of the Royal Astronomical Society*, 351(1):169–185, 2004.

[9] Edward M Cackett. *Compact objects in active galactic nuclei and X-ray binaries.* PhD thesis, University of St Andrews, 2007.

[10] Donald E Osterbrock and Gary J Ferland. *Astrophysics Of Gas Nebulae and Active Galactic Nuclei.* University science books, 2006.

[11] P Hartigan, A Frank, JM Foster, BH Wilde, M Douglas, PA Rosen, RF Coker, BE Blue, and JF Hansen. Fluid dynamics of stellar jets in real time: Third epoch hubble space telescope images of hh 1, hh 34, and hh 47. *The Astrophysical Journal*, 736(1):29, 2011.

[12] Julian H Krolik. *Active galactic nuclei: from the central black hole to the galactic environment*, volume 10. Princeton University Press, 1999.

[13] V. Beckmann, U. Lidzén, S. Vaughan, N. Gehrels, S. Soldi, V. A. Dogiel, and R. G. Petrov. Active galactic nuclei. *European Physical Journal H*, 37(1):185–233, 2009.

[14] Chiara Feruglio, Roberto Maiolino, Enrico Piconcelli, Nicola Menci, Herve' Aussel, Alessandra Lamastra, and Fabrizio Fiore. Quasar feedback revealed by giant molecular outflows. *Astronomy & Astrophysics*, 518:L155, 2010.

[15] Bradley M Peterson. *An introduction to active galactic nuclei.* Cambridge University Press, 1997.

[16] C Megan Urry and Paolo Padovani. Unified schemes for radio-loud active galactic nuclei. *Publications of the Astronomical Society of the Pacific*, 107(715):803, 1995.

[17] H Netzer. Active galactic nuclei: Basic physics and main components, 2006.

[18] L.S Sparke and J.S. *Galaxies in the Universe: An introduction.* Cambridge University press, 2007.

[19] Paolo Padovani, DM Alexander, RJ Assef, B De Marco, P Giommi, RC Hickox, GT Richards, V Smolčić, E Hatziminaoglou, V Mainieri, et al. Active galactic nuclei: what's in a name? *The Astronomy and Astrophysics Review*, 25:1–91, 2017.

[20] Hannu Karttunen, Pekka Kröger, Heikki Oja, Markku Poutanen, and Karl Johan Donner. *Fundamental astronomy.* Springer, 2007.

[21] Hong-Yee Chiu. Gravitational collapse. *American Journal of Physics*, 32(10):783–785, 1964.

[22] J. M. Fanaroff, B. L. & Riley. The morphology of distant radio galaxies. *Monthly Notices of the Royal Astronomical Society*, 167:31P, 1974.

[23] S. Kellermann, K. I. & Rawlings. Imaging the universe: From the centimeter to the ultraviolet using interferometry. *Annual Review of Astronomy and Astrophysics*, 54(1):117–154, 2016.

[24] S. Courteau, R. B. Tully, and D. I. Makarov. Nearby galaxies: The distance to the andromeda galaxy and the combined mass of our local group. *Nature*, 511(7511):193–197, 2014.

[25] G. Ghisellini, F. Tavecchio, and R. D. Blandford. Jets in blazars. *Monthly Notices of the Royal Astronomical Society*, 407(2):655–688, 2010.

[26] KII Koljonen, KS Long, JH Matthews, and C Knigge. The origin of optical emission lines in the soft state of x-ray binary outbursts: the case of maxi j1820+ 070. *Monthly Notices of the Royal Astronomical Society*, 521(3):4190–4206, 2023.

[27] Dipanweeta Bhattacharyya and Arun Mangalam. Cosmic spin and mass evolution of black holes and its impact. *The Astrophysical Journal*, 895(2):130, 2020.

[28] Robert Antonucci. Unified models for active galactic nuclei and quasars. *Annual review of astronomy and astrophysics*, 31(1):473–521, 1993.

[29] Enrico Ramirez-Ruiz, Annalisa Celotti, and Martin J Rees. Events in the life of a cocoon surrounding a light, collapsar jet. *Monthly Notices of the Royal Astronomical Society*, 337(4):1349–1356, 2002.

[30] P. F. Hopkins, L. Hernquist, T. J. Cox, and et al. The stellar mass content of active galactic nuclei hosts as measured by their near-infrared luminosities. *The Astrophysical Journal*, 599(2):955–970, 2003.

[31] Marko Stalevski. Investigating the structure of active galactic nuclei: the dusty torus, 2012.

[32] Yerbol Khassen. Active galactic nuclei. *arXiv preprint arXiv:1010.6281*, 2010.

[33] Nicolai Ivanovich Shakura and Rashid Alievich Sunyaev. Black holes in binary systems. observational appearance. *Astronomy and Astrophysics, Vol. 24, p. 337-355*, 24:337–355, 1973.

[34] Bradley M Peterson. Variability of active galactic nuclei. In *Advanced Lectures on the Starburst-AGN Connection*, pages 3–68. World Scientific, 2001.

[35] Mara Salvato. Rosat bright survey: Seyfert 1 host galaxies and their environment. *Ph. D. Thesis*, 2002.

[36] Michele Cappellari, Alvio Renzini, Laura Greggio, Sperello di Serego Alighieri, Lucio M Buson, David Burstein, and Francesco Bertola. The mini-active galactic nucleus at the center of the elliptical galaxy ngc 4552 with hubble space telescope. *The Astrophysical Journal*, 519(1):117, 1999.

[37] Tommaso Freschi. The correlation between the luminosity of active galactic nuclei and host galaxy parameters.

[38] Mark Lacy and Anna Sajina. Active galactic nuclei as seen by the spitzer space telescope. *Nature Astronomy*, 4(4):352–363, 2020.

[39] Li-Xin Li, Ramesh Narayan, and Jeffrey E McClintock. Inferring the inclination of a black hole accretion disk from observations of its polarized continuum radiation. *The Astrophysical Journal*, 691(1):847, 2009.

[40] N. I. Shakura and R. A. Sunyaev. Black holes in binary systems. observational appearance. *Astron. Astrophys.*, 24:337–347, 1973.

[41] A. C. Fabian and M. J. Rees. Accretion onto black holes: Observations and theory. *Space Science Reviews*, 169(1).

[42] George B Rybicki and Alan P Lightman. *Radiative processes in astrophysics.* John Wiley & Sons, 1991.

[43] Feng Yuan and Ramesh Narayan. Hot accretion flows around black holes. *Annual Review of Astronomy and Astrophysics*, 52:529–588, 2014.

[44] Michael S. Shull and Peter B. Stetson. Nhe2-mediated bicarbonate reabsorption in the rat proximal tubule: Stochastic modeling and luminal bicarbonate concentration dependence. *Journal of Clinical Investigation*, 85(6):1785–1792, 1990.

[45] C Martin Gaskell and René W Goosmann. Line shifts, broad-line region inflow, and the feeding of active galactic nuclei. *The Astrophysical Journal*, 769(1):30, 2013.

[46] Roger D. Blandford and David L. Meier. Fluid dynamics and magnetic fields in extragalactic radio sources. *Annual Review of Astronomy and Astrophysics*, 52(1):161–201, 2014.

[47] M. C. Begelman, A. C. Fabian, and M. J. Rees. Constraints on the location of the broad-line region in active galactic nuclei. *Monthly Notices of the Royal Astronomical Society*, 387(4):1649–1659, 2008.

[48] M. Sikora, M. Nalewajko, and G. Madejski. On the significance of relativistically hot pairs in the jets of fr ii radio galaxies. *ApJ*, 777(1), 2013.

[49] E. J. Murphy, A. D. Myers, M. A. Dopita, and J.-H. Choi. Star-forming dwarf galaxies: The correlation between far-infrared and radio fluxes. *ApJ*, 768(21), 2013.

[50] A. Gould and T. M. Walker. Microlensing searches for dark matter. *ApJ*, 414:L27–L30, 1993.

[51] B. D. Savage and K. R. Sembach. Intrinsic column densities of interstellar gas toward distant quasars. *ApJ*, 379:245–272, 1991.

[52] R. Ganguly and M. S. Brotherton. Hs 1700+6416: the first high-redshift unlensed narrow absorption line-qso showing variable high-velocity outflows. *ApJ*, 672(1):102.

[53] Bruce T. Draine. Interstellar dust grains. *Annual Review of Astronomy and Astrophysics*, 41:241–289, 2003.

[54] Robert Antonucci. Unified models for active galactic nuclei and quasars. *ApJ*, 417:472–489, 1993.

[55] M. Nenkova, A. Sirotti, N. Nikolov, and Z. Ivezic. Spitzer spectroscopy of infrared-detected agns. i. silicate absorption and the origin of the mid-infrared emission. *ApJ*, 685(1):160.

[56] Michael A. Dopita and Ralph S. Sutherland. *Astrophysics of the Diffuse Universe*. Springer, 2007.

[57] BT Draine and Aigen Li. Infrared emission from interstellar dust. iv. the silicate-graphite-pah model in the post-spitzer era. *The Astrophysical Journal*, 657(2):810, 2007.

[58] N. Siegel, S. R. Majewski, R. D. Blum, and O. Hahn. A wide-field near-infrared survey of the magellanic clouds. ii. the color-magnitude distribution and luminosity function of the lmc. *ApJ*, 543(1):608.

[59] Álvaro Villalobos, Gabriella De Lucia, and Giuseppe Murante. Simulating the evolution of disc galaxies in a group environment–ii. the influence of close encounters between galaxies. *Monthly Notices of the Royal Astronomical Society*, 444(1):313–326, 2014.

[60] BR McNamara and PEJ Nulsen. Heating hot atmospheres with active galactic nuclei. *Annu. Rev. Astron. Astrophys.*, 45:117–175, 2007.

[61] Rachel S Somerville, Philip F Hopkins, Thomas J Cox, Brant E Robertson, and Lars Hernquist. A semi-analytic model for the co-evolution of galaxies, black holes and active galactic nuclei. *Monthly Notices of the Royal Astronomical Society*, 391(2):481–506, 2008.

[62] Guinevere Kauffmann, Timothy M Heckman, Christy Tremonti, Jarle Brinchmann, Stéphane Charlot, Simon DM White, Susan E Ridgway, Jon Brinkmann, Masataka Fukugita, Patrick B Hall, et al. The host galaxies of active galactic nuclei. *Monthly Notices of the Royal Astronomical Society*, 346(4):1055–1077, 2003.

[63] Rogério Riffel, Nicolas D Mallmann, Sandro B Rembold, Gabriele S Ilha, Rogemar A Riffel, Thaisa Storchi-Bergmann, Daniel Ruschel-Dutra, Alexandre

Vazdekis, Ignacio Martín-Navarro, Jaderson S Schimoia, et al. Mapping the stellar population and gas excitation of manga galaxies with megacubes. results for agn versus control sample. *Monthly Notices of the Royal Astronomical Society*, 524(4):5640–5657, 2023.

[64] John Kormendy and Douglas Richstone. Inward bound—the search for supermassive black holes in galactic nuclei. *Annual review of astronomy and Astrophysics*, 33(1):581–624, 1995.

[65] Laura Ferrarese and Holland Ford. Supermassive black holes in galactic nuclei: past, present and future research. *Space Science Reviews*, 116(3-4):523–624, 2005.

[66] Charles W Misner, Kip S Thorne, and John Archibald Wheeler. *Gravitation*. Macmillan, 1973.

[67] Malcolm AH MacCallum. Exact solutions of einstein's equations. *Scholarpedia*, 8(12):8584, 2013.

[68] Bernard Schutz. *A first course in general relativity*. Cambridge university press, 2022.

[69] Karl Schwarzschild. Über das gravitationsfeld eines massenpunktes nach der einsteinschen theorie. *Sitzungsberichte der Königlich Preußischen Akademie der Wissenschaften*, pages 189–196, 1916.

[70] Sean M. Carroll. *Spacetime and Geometry: An Introduction to General Relativity*, volume 1. Addison-Wesley, New York, 2004.

[71] Jonatan Nordebo. The reissner-nordström metric, 2016.

[72] Roy P Kerr. Gravitational field of a spinning mass as an example of algebraically special metrics. *Physical review letters*, 11(5):237, 1963.

[73] Fulvio Melia. *Cracking the Einstein Code: relativity and the birth of black hole physics*. University of Chicago Press, 2020.

[74] Albert Snepppen. Divergent reflections around the photon sphere of a black hole. *Scientific reports*, 11(1):14247, 2021.

[75] Ezra T Newman and AI Janis. Note on the kerr spinning-particle metric. *Journal of Mathematical Physics*, 6(6):915–917, 1965.

[76] Tim Adamo and Ezra T Newman. The kerr-newman metric: a review. *arXiv preprint arXiv:1410.6626*, 2014.

[77] B. Kent Harrison. Bäcklund transformation for the ernst equation of general relativity. *Phys. Rev. Lett.*, 41:1197–1200, Oct 1978.

[78] Yu-Ching Chou. A radiating kerr black hole and hawking radiation. *Heliyon*, 6(1), 2020.

[79] Lev D Landau and Evgeny M Lifshitz. *Course of theoretical physics*. Butterworth-Heinemann, 1975.

[80] George B. Rybicki and Alan P. Lightman. *Radiative Transfer in Scattering and Absorbing Atmospheres*. Random House, 1979.

[81] Steven Von Fuerst. *General relativistic radiative transfer*. University of London, University College London (United Kingdom), 2006.

[82] Hung-Yi Pu, Kiyun Yun, Ziri Younsi, and Suk-Jin Yoon. Odyssey: a public gpu-based code for general relativistic radiative transfer in kerr spacetime. *The Astrophysical Journal*, 820(2):105, 2016.

[83] Mattias Marklund and CA Clarkson. The general relativistic magnetohydrodynamic dynamo equation. *Monthly Notices of the Royal Astronomical Society*, 358(3):892–900, 2005.

[84] M Kozlowski, M Jaroszynski, and MA Abramowicz. The analytic theory of fluid disks orbiting the kerr black hole. *Astronomy and Astrophysics, vol. 63, no. 1-2, Feb. 1978, p. 209-220. Research supported by the Universita di Padova.*, 63:209–220, 1978.

[85] Luciano Rezzolla and Olindo Zanotti. *Relativistic hydrodynamics*. Oxford University Press, USA, 2013.

[86] E. Tejeda and S. Rosswog. Gravitational time dilation in binary neutron star mergers. *Monthly Notices of the Royal Astronomical Society*, 433(2):1930–1937, 2013.

[87] James M. Bardeen and Jacobus A. Petterson. The lense-thirring effect and accretion disks around kerr black holes. *The Astrophysical Journal*, 195:L65–L67, 1975.

[88] V. Bozza. Gravitational lensing by black holes. *General Relativity and Gravitation*, 42(9):2269–2300, 2008.

[89] I. D. Novikov and K. S. Thorne. *Astrophysics of black holes.* Gordon and Breach, 1973.

[90] Juhan Frank, Andrew R King, and Derek Raine. *Accretion power in astrophysics.* Cambridge university press, 2002.

[91] Andrea M Ghez, S Salim, NN Weinberg, JR Lu, Tea Do, JK Dunn, K Matthews, MR Morris, S Yelda, EE Becklin, et al. Measuring distance and properties of the milky way's central supermassive black hole with stellar orbits. *The Astrophysical Journal*, 689(2):1044, 2008.

[92] Peter J Mohr, Barry N Taylor, and David B Newell. Codata recommended values of the fundamental physical constants: 2006. *Journal of Physical and Chemical Reference Data*, 37(3):1187–1284, 2008.

[93] Kip S Thorne. Disk-accretion onto a black hole. ii. evolution of the hole. *Astrophysical Journal, Vol. 191, pp. 507-520 (1974)*, 191:507–520, 1974.

[94] Malcolm S. Longair. *High Energy Astrophysics.* Cambridge University Press, 2011.

[95] Andrzej G. Pacholczyk. *Radio Astrophysics: Nonthermal Processes in Galactic and Extragalactic Sources.* Freeman, 1970.

[96] Rebecca J. Ickox and David M. Alexander. The energetic impact of active galactic nuclei. *Annual Review of Astronomy and Astrophysics*, 56:625–671, 2018.

[97] Rainer Siebenmorgen, Fabian Heymann, and Andreas Efstathiou. Sed library of agn torus models. *ESO Messenger*, 177:26–30, 2015.

[98] Bernard A. et al. Lippmann. *Introduction to electrodynamics and optics.* Oxford University Press, 2003.

**JIMMA UNIVERSITY**

**COLLAGE OF NATURAL SCIENCES**

**PERFORMANNCE CERTIFICATE FOR MASTER'S DEGREE**

Name of Student: Mihiret Mekonen

Graduate Program: MSc Regular

ID No.: RM0719/15-0

1. Course Work Performance Excellent, Very Good, Good, Satisfactory, Fail.

| Course Code | Course Title | Cr.hr | Score(100) | Grade | Rank | Remark |
|---|---|---|---|---|---|---|
| Phys 799 | Graduate Thesis | 6 | | | | |

Thesis Title: **HYDRODYNAMIC RADIATIVE TRANSFER PROCESS AROUND ACTIVE GALACTIC NUCLEI**

2. Board of Examiners decision Mark X in one of the boxes. Pass □ Failed □

If failed, give reasons and indicate plans for re-examination.

______________________________________________

______________________________________________

______________________________________________

____________________-

3. Approved by:

| Committee member | Name | Sign | Date |
|---|---|---|---|
| Chairman | ________________________- | _________ | ______________- |
| External Examiner | ________________________- | _________ | ______________- |
| Internal Examiner | ________________________- | _________ | ______________- |
| Major Advisor | ________________________- | _________ | ______________- |
| Department Head | ________________________- | _________ | ______________- |

**School of Graduate Studies**

**Jimma University**

**College of Natural Sciences**

**MSc. Thesis Approval Sheet**

We the undersigned, member of the Board of Examiners of the final open defense by Mihiret Mekonen have read and evaluated his thesis entitled **HYDRODYNAMIC RADIATIVE TRANSFER PROCESS AROUND ACTIVE GALACTIC NUCLEI** and examined the candidate. This is therefore to certify that the thesis has been accepted in partial fulfillment of the requirements for the degree Master of Science in Physics (ASTROPHYSICS).

| Committee member | Name | Sign | Date |
| --- | --- | --- | --- |
| Chairman | ____________________ | ________ | ____________- |
| External Examiner | ____________________ | ________ | ____________- |
| Internal Examiner | ____________________ | ________ | ____________- |
| Major Advisor | ____________________ | ________ | ____________- |
| Department Head | ____________________ | ________ | ____________- |

**School of Graduate Studies**

**Graduate Thesis Ownership Agreement**

This thesis is a property of Jimma university, an institution that awarded MSc Degree to the graduate student and funded its research cost fully or partly. The research work was accomplished under the close support and supervision of the assigned university's academic staff. It is therefore strictly forbidden to publish, modify or communicate to or put at the disposal of third party the entire document or any part thereof with out the common consent of the research supervisor(s) and the graduate. Disregarding this agreement would lead to accountability according to the Jimma university's Research and publication Misconduct policy Article 1.7 of the university's Document for "Guidelines and procedures for Research, July 2022".

| Name of Graduate student | Signature | Date |
|---|---|---|
| Mihiret mekonen | | |

| Name of the Research Advisor | Signature | Date |
|---|---|---|
| Tolu Birresa (PhD) | | |

Thesis Title: HYDRODYNAMIC RADIATIVE TRANSFER PROCESS AROUND ACTIVE GALACTIC NUCLIE

Degree Awarded: **MSc**